Development 140, 1621-1638 (2013) doi:10.1242/dev.083519

Morphogen transport

Patrick Müller[1,*,‡], Katherine W. Rogers[1], Shuizi R. Yu[2,3], Michael Brand[2,3] and Alexander F. Schier[1,4,‡]

Summary

The graded distribution of morphogens underlies many of the tissue patterns that form during development. How morphogens disperse from a localized source and how gradients in the target tissue form has been under debate for decades. Recent imaging studies and biophysical measurements have provided evidence for various morphogen transport models ranging from passive mechanisms, such as free or hindered extracellular diffusion, to cell-based dispersal by transcytosis or cytonemes. Here, we analyze these transport models using the morphogens Nodal, fibroblast growth factor and Decapentaplegic as case studies. We propose that most of the available data support the idea that morphogen gradients form by diffusion that is hindered by tortuosity and binding to extracellular molecules.

Key words: Morphogen, Gradient, Diffusion, Cytoneme, Signaling

Introduction

For more than a century, gradients of signaling molecules have been proposed to direct the formation of tissues during embryogenesis (Morgan, 1901; Turing, 1952; Stumpf, 1966; Wolpert, 1969; Crick, 1970) (reviewed by Rogers and Schier, 2011). The idea of such signaling gradients emerged following observations that some cells can induce the formation of structures in neighboring tissues. This led to the hypothesis that signaling molecules, termed morphogens, are produced at a localized source and disperse in the target tissue. The resulting morphogen concentration gradient dictates the expression of different sets of genes and leads to tissue patterning and morphogenesis. Morphogens act over different distances (tens to hundreds of micrometers) and different times (hours to days) in different developmental contexts, from patterning wing precursors in flies to inducing and patterning germ layers in vertebrate embryos (reviewed by Rogers and Schier, 2011). However, neither the non-autonomous function of morphogens nor their graded distributions and different signaling ranges directly implicate a specific transport mechanism.

Several models have been proposed to explain how morphogens move from their source to target tissues. Here, we analyze recent studies and models of morphogen transport and discuss whether there is a dominant mode of movement. Current transport models can be broadly grouped into: (1) extracellular diffusion-based mechanisms; and (2) cell-based mechanisms, in which morphogens move through cells or along cellular extensions. We first lay out three diffusion-based models for extracellular morphogen transport (free, hindered and facilitated diffusion) and two cell-based mechanisms (transcytosis and cytoneme-mediated transport). We use mathematical modeling and the classic analogy of a 'drunken sailor' to illustrate the principles behind each model. Next, we analyze recent experiments that have examined morphogen movement and discuss evidence for and against each transport model, focusing on the morphogens Nodal, fibroblast growth factor (FGF) and Decapentaplegic (Dpp). Based on this analysis, we hypothesize that most of the available data are consistent with diffusion models, in which hindrance due to tortuosity and binding interactions is often considerable. We end by suggesting future research directions to resolve the current debates regarding morphogen transport.

Theories of morphogen transport

Morphogens move from the site where they are produced (the source) through complex environments, leading to the formation of a morphogen gradient in the target tissue (Fig. 1A). Models of morphogen transport therefore frequently involve complex mathematical descriptions that include several coupled partial differential equations. In simplified terms, these models can be illustrated by the 'drunken sailor' analogy (Fig. 1) (Pearson, 1905a; Pearson, 1905b; Rayleigh, 1905; Stewart, 2001). In this analogy, a ship (source) loaded with drunken sailors (morphogen molecules) arrives at the harbor of a city (target tissue). The path of a disembarking drunken sailor moving into the city illustrates the random walk of each molecule as it moves through the target tissue (Fig. 1B, inset). Each drunken sailor walks with a certain average step size and moves in a random direction with each step. This analogy reflects the diffusive behavior of molecules as they bounce off each other and change direction.

Various models explaining the transport of morphogens can thus be described in terms of the drunken sailor analogy. In the following sections, we discuss five major models: (1) free diffusion, i.e. drunken sailors performing purely random walks (Fig. 1B); (2) tortuosity- and binding-mediated hindered diffusion, i.e. drunken sailors walking around buildings (Fig. 1C) and visiting pubs (Fig. 1D); (3) facilitated diffusion, i.e. drunken sailors prevented from visiting pubs by police officers (Fig. 1E,F); (4) transcytosis, i.e. drunken sailors walking through buildings (Fig. 1G); and (5) directed transport via filopodial extensions called cytonemes, i.e. drunken sailors transported through subway tunnels (Fig. 1H).

Transport model 1: free diffusion

In the simplest case of morphogen dispersal, molecules move by 'free diffusion' (see Glossary, Box 1) from the source to the target tissue. In the drunken sailor analogy, each sailor performs a random walk (Fig. 1B, inset). The dynamics of dispersal can be described by the diffusion coefficient *D*. However, free diffusion is not sufficient for gradient formation: if sailors simply moved by free diffusion, they would eventually be distributed evenly in the city [i.e. a nearly uniform distribution of morphogen molecules would

[1]Department of Molecular and Cellular Biology, Harvard University, Cambridge, MA 02138, USA. [2]Developmental Genetics, Biotechnology Center, TUD, 01307 Dresden, Germany. [3]Center for Regenerative Therapies, TUD, 01307 Dresden, Germany. [4]FAS Center for Systems Biology, Harvard University, Cambridge, MA 02138, USA.

*Present address: Max Planck Institute for Developmental Biology, Spemannstraβe 35, 72076 Tübingen, Germany
‡Authors for correspondence (pmueller@tuebingen.mpg.de; schier@fas.harvard.edu)

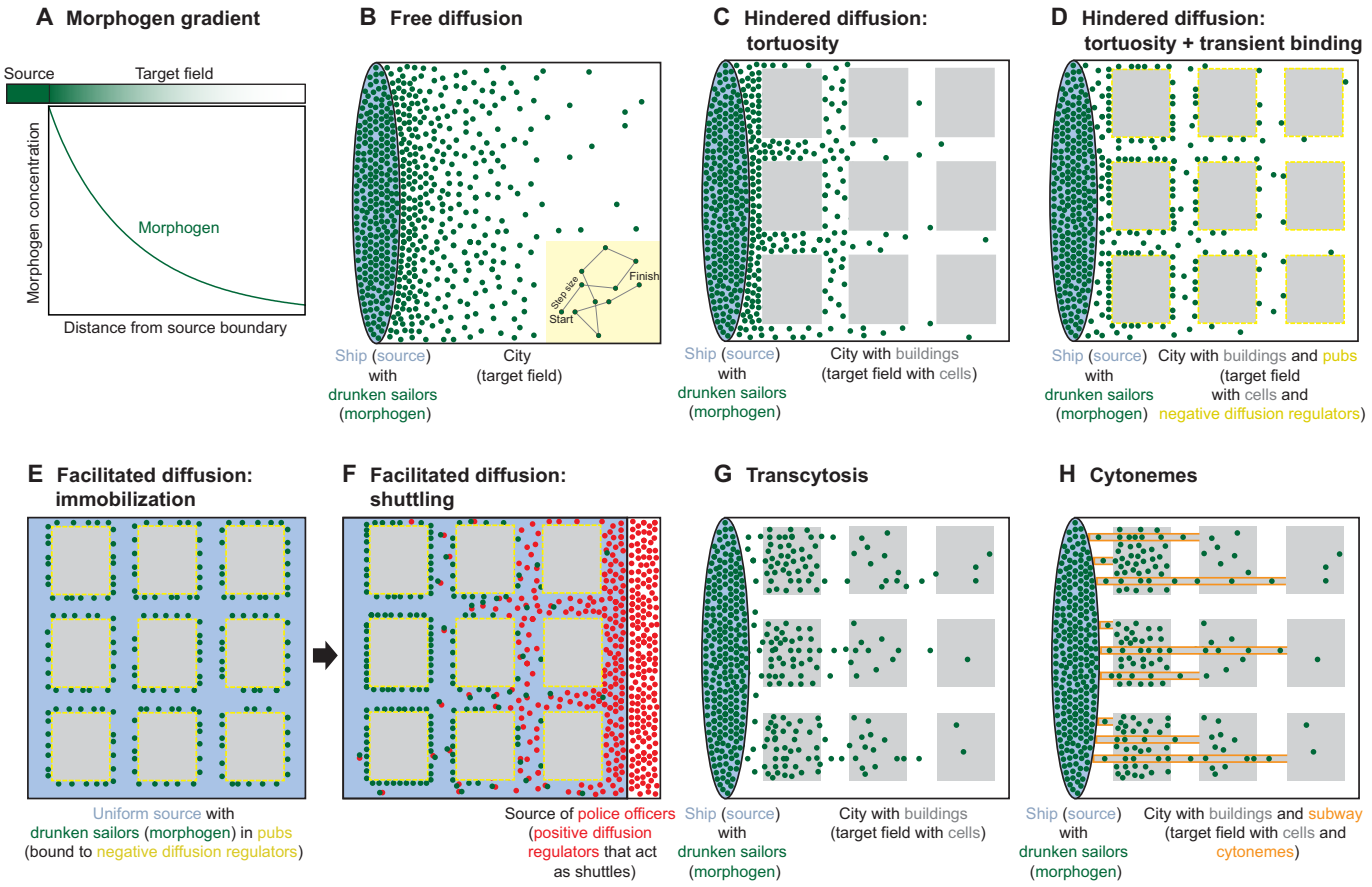

Fig. 1. Morphogen transport and the drunken sailor analogy. (**A**) The transport of morphogens from a source establishes a gradient in the target field. (B-H) Five major morphogen transport models are illustrated using the drunken sailor analogy, in which drunken sailors move by random walks from a ship into a city. In this analogy, morphogen molecules are represented by sailors and cells are represented by buildings. (**B**) In the case of free diffusion, sailors (green dots) leave the ship (blue oval) and disperse into the city (white square). Inset: sailors take steps of the indicated fixed size and the direction of each step is random. This 'random walk' describes the diffusive behavior of molecules in solution. (**C**) In the tortuosity-mediated hindered diffusion model, buildings (gray) act as obstacles that sailors must move around, thus increasing the tortuosity of the environment. (**D**) In the case of diffusion that is hindered by tortuosity and transient binding, the sailors stop in pubs (negative diffusion regulators, yellow) located at the periphery of buildings. Note that, in contrast to effects from tortuosity alone, sailors congregate at the periphery of buildings, and there are relatively few freely moving sailors. (**E**,**F**) The shuttling model does not require a localized source of sailors. Instead, sailors are initially present mostly in pubs (negative diffusion regulators, yellow) and uniformly distributed in the city (E). Police officers (positive diffusion regulators, red) disperse from a source on the right side, pick up sailors from pubs and escort them through the city by preventing further pub visits (F). When police officers disappear (not shown), sailors can re-enter the pubs. Over time, this results in the concentration of sailors on the left. (**G**) In the transcytosis model, the sailors travel through the buildings. (**H**) During directed transport mediated by cytonemes, the sailors travel through subway tunnels (orange), which deposit the sailors in buildings.

be seen in the target tissue (Wartlick et al., 2009)]. For a gradient to form, some drunken sailors need to disappear along the way; a sailor might die (i.e. the morphogen is degraded) or he may enter and remain in a building (i.e. the morphogen is permanently trapped by a cell). Both events remove sailors/molecules from the mobile pool and are therefore referred to as 'clearance' (see Glossary, Box 1). The combination of drunken sailors constantly disembarking from the ship (production), moving through the city (diffusion) and disappearing (clearance) along the way results in the graded distribution of sailors in the city over time (Fig. 1B) (Crick, 1970; Lander et al., 2002; Wartlick et al., 2009; Yu et al., 2009; Zhou et al., 2012). For a detailed mathematical model of free diffusion, see Fig. 2A.

The free diffusion model makes four major predictions. First, morphogens move by extracellular diffusion. Second, morphogens have a high free 'diffusivity' (see Glossary, Box 1) that is described by the Einstein-Stokes relationship (Berg, 1993; Müller and Schier, 2011). The diffusion coefficient should thus be close to theoretical predictions based on the size of the morphogen and the properties of its environment. Third, to allow for gradient formation, morphogen clearance is fast relative to diffusion (Yu et al., 2009; Zhou et al., 2012). Clearance could be achieved by rapid degradation, in which case the molecules have a short lifetime, or by rapid permanent immobilization on or in target cells. In the latter case, the fraction of freely moving molecules is small because most morphogen molecules are permanently trapped (Fig. 2A). Fourth, gradient formation kinetics are rapid; the gradient shape is established early and does not change (Fig. 2C). By contrast, the amplitude of the gradient increases if the immobilized molecules have a long lifetime (Fig. 2A).

Transport model 2: hindered diffusion

In a related model of morphogen transport, 'hindered diffusion' (see Glossary, Box 1), the extracellular diffusion of molecules is

Box 1. Glossary

Clearance. The removal of morphogen from the mobile pool by degradation or trapping due to permanent immobilization at the cell surface or permanent cellular uptake.

Diffusivity. Also referred to as 'diffusion coefficient', 'diffusion constant' or 'diffusion rate', this constant describes how fast a population of molecules spreads. A high value indicates fast spreading, whereas a low value indicates slow spreading.

Diffusion regulator. Molecules that interact with morphogens and affect their diffusion. Interactions with diffusion regulators may decrease or increase effective diffusivity. In the hindered diffusion model, transient binding to 'negative' diffusion regulators on the cell surface reduces effective diffusivity, whereas in the facilitated diffusion model 'positive' diffusion regulators enhance effective diffusivity.

Effective diffusion. This type of diffusion, which is also referred to as 'global diffusivity', takes into account multi-scale effects such as tortuosity and transient binding. The effective diffusivity of a particle moving through and interacting with a complex environment is typically lower than the free diffusivity of the same particle in solution (Kicheva et al., 2012b).

Facilitated diffusion. The enhancement of morphogen diffusivity by a 'positive' diffusion regulator. For example, morphogen binding to a positive diffusion regulator may inhibit interactions with cell surfaces that would otherwise hinder morphogen movement.

Free diffusion. The spreading of particles by random walks in solution in the absence of cells or other obstacles. The mean squared displacement of the population of particles is proportional to the diffusion coefficient multiplied by time. This type of diffusion is also referred to as 'molecular diffusion' and is dependent on the size of the diffusing molecule as well as the temperature and viscosity of the surrounding medium (Berg, 1993; Müller and Schier, 2011).

Hindered diffusion. Diffusion that is hindered by geometric obstacles, causing an increase in the path length that molecules have to travel, or by transient binding to immobilized molecules.

Local diffusivity. The diffusion coefficient that describes the diffusion of molecules in a small, localized volume and does not take into account global effects on movement.

Steady state. In the context of morphogen gradient formation, a gradient has reached steady state when the concentration in space no longer observably changes over time. Note that it is possible to define steady state in terms of the gradient shape as well; the shape of the gradient reaches steady state when the change in concentration in space no longer observably changes over time. Assuming localized constant production, diffusion and uniform clearance, the steady state of gradient shape is determined by the morphogen's effective diffusivity and clearance, whereas the steady state of gradient amplitude also takes into account the lifetime of the cleared morphogen. Thus, gradient shape may reach steady state before the gradient amplitude (Fig. 2).

hindered by obstacles (tortuosity-mediated hindrance) and by transient binding interactions (binding-mediated hindrance). Relating back to the drunken sailor analogy, each sailor walks through the streets of a city around buildings and transiently enters and leaves pubs along the way. Similar to the free diffusion model, morphogens undergo random walks but walks are restricted by cells and interrupted by extracellular binding interactions.

Tortuosity-mediated hindrance

Tissues are often densely packed with cells. In contrast to the free diffusion model, which posits that geometric effects from cells on diffusion are negligible or that movement occurs outside of the cell field, hindered diffusion postulates that cell packing, and hence tortuosity (see Box 2), strongly influences the movement of extracellular molecules. Extracellular morphogens must go around cells and this reduces their overall dispersal (Nicholson and Syková, 1998; Rusakov and Kullmann, 1998; Nicholson, 2001; Tao and Nicholson, 2004; Thorne and Nicholson, 2006; Thorne et al., 2008). In the drunken sailor analogy, sailors perform random walks in a region containing buildings, not in a large empty lot (Fig. 1C). Although the local movements and step sizes of the sailors are identical in both scenarios, it will take sailors, on average, longer to travel a given distance in the packed region (see Box 2). Thus, in a cellular environment, the 'local' extracellular diffusion coefficient (or 'local diffusivity', see Glossary, Box 1) is similar to free diffusivity, whereas the 'effective diffusion' (see Glossary, Box 1) coefficient (or 'global diffusivity') is reduced.

Binding-mediated hindrance

In addition to geometric hindrance mediated by cellular obstacles, morphogen movement might be further hindered by transient binding to extracellular molecules, such as morphogen receptors or extracellular matrix components (Crank, 1979; Lander et al., 2002; Baeg et al., 2004; Belenkaya et al., 2004; Han et al., 2004; Lin, 2004; Han et al., 2005; Callejo et al., 2006; Hufnagel et al., 2006; Thorne et al., 2008; Wang et al., 2008; Miura et al., 2009; Yan and Lin, 2009; Müller and Schier, 2011; Müller et al., 2012; Sawala et al., 2012). In the drunken sailor analogy, sailors frequently linger in pubs along the way (Fig. 1D). The local 'speed' of sailors moving between pubs is the same as in the free diffusion model, but their residence time in pubs reduces their global 'speed' of moving through the city. Thus, binding-mediated hindrance of morphogens will reduce the effective diffusion coefficient. For a detailed mathematical model of binding-mediated hindered diffusion, see Fig. 2B.

The key predictions of the binding-mediated hindered diffusion model are as follows. First, morphogens move through extracellular diffusion. Second, the effective diffusion coefficient is lower than the free diffusion coefficient because morphogens transiently bind to extracellular immobilized molecules ('diffusion regulators', see Glossary, Box 1). Third, the number of freely moving molecules is expected to be small because most morphogen molecules would be bound to diffusion regulators at any given point in time (Fig. 2B). Fourth, in contrast to the free diffusion model, the clearance of morphogen does not need to be rapid; because global diffusion is slow, gradients can form even when mobile molecules are long-lived. Fifth, gradient shape evolves more slowly over time than in the free diffusion model due to slower overall dispersal of the morphogen (Fig. 2C). As in the free diffusion model, the amplitude of the gradient increases over time if the cleared molecules have a long lifetime (Fig. 2B).

Notably, the free and hindered diffusion models can eventually lead to the same 'steady state' (see Glossary, Box 1) morphogen gradient (Fig. 2A,B), but the kinetics of gradient formation are different (Fig. 2C). This distinction is particularly relevant in rapidly developing systems in which gradients might be interpreted quickly or might not reach steady state.

Transport model 3: facilitated diffusion and shuttling

Models based on 'facilitated diffusion' (see Glossary, Box 1) are an extension of hindered diffusion models, in which morphogen movement is enhanced by interactions with 'positive' diffusion regulators that release the hindrance exerted by 'negative' diffusion regulators. In this scenario, the morphogen is largely immobile until bound to a positive diffusion regulator that enhances its

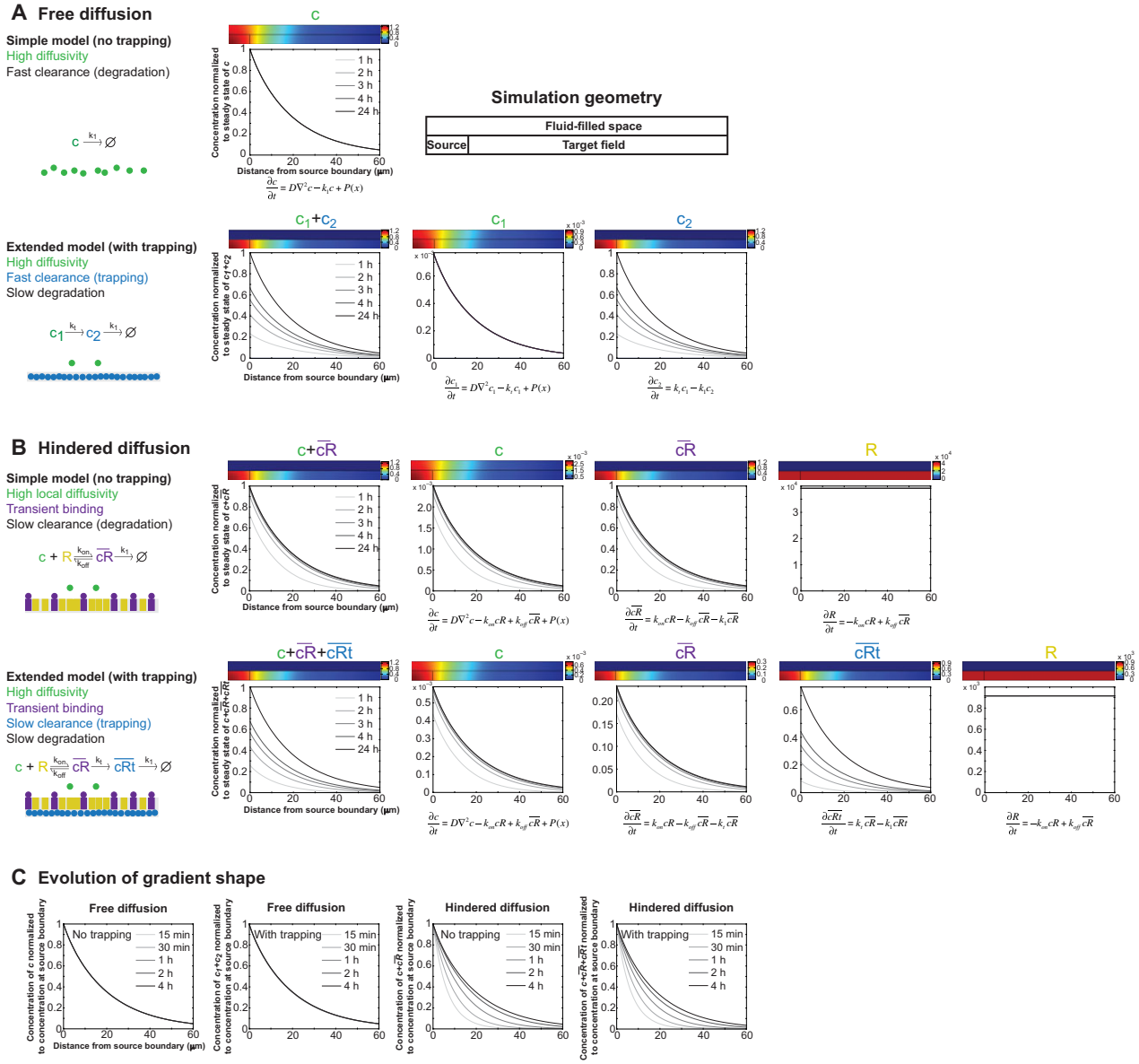

Fig. 2. Gradient formation in models of free diffusion and hindered diffusion. A tissue layer with overlying fluid-filled space covered by a non-responsive roof is used to illustrate the behavior of different diffusion models. This geometry is similar to that found in the *Drosophila* wing disc (Kornberg and Guha, 2007). Production [$P(x)$] only occurs in the source, diffusion occurs everywhere, and other reactions are restricted to the source and target field. All models lead to a similar steady state distribution of morphogen in the target field. (**A**) Free diffusion. In the simplest model, morphogen (c; green) is produced, diffuses freely with diffusivity D, and is degraded rapidly with a clearance rate constant k_1. The gradient of c rapidly reaches steady state. In an extended model, c_1 is cleared rapidly by trapping (irreversible binding or cellular uptake), converting c_1 into an immobile population c_2, which is degraded slowly with the degradation rate constant k_1. The immobilized species (c_2; blue) rather than the extracellular species (c_1; green) dominates the slow gradient formation dynamics. (**B**) In the binding-mediated hindered diffusion model, morphogen diffuses and transiently binds to immobilized diffusion regulators (R; yellow). Thus, although molecules have high local diffusivities, their effective global diffusivity is low. The majority of morphogen is present in a form that is bound to diffusion regulators ($\overline{cR}$; purple), which leads to the concentration of morphogen in the tissue layer and to exclusion from the fluid-filled space. In an extended model, $\overline{cR}$ is converted into an irreversibly trapped fraction, $\overline{cRt}$, with a clearance rate constant k_t. $\overline{cRt}$ is degraded with a degradation rate constant k_1. In both the free and hindered diffusion models, the free extracellular concentration of morphogens is low. (**C**) The free and hindered diffusion models can lead to the same steady state morphogen distribution but predict distinct gradient formation kinetics. The free diffusion model predicts rapid progression to the final shape of the distribution, whereas hindered diffusion models predict slow progression. Shown are the curves from the first graphs in A and B normalized to the respective concentrations at the source boundary. Simulations were performed similar to those of Müller et al. (Müller et al., 2012) using a two-dimensional geometry of 200 μm length and 12 μm height; source width of 10 μm; fluid-filled space height of 6 μm; no-flux boundary conditions; initial morphogen concentrations of zero; concentration gradients were sampled in the middle of the target field at a height of 3 μm. Parameters used: (A) simple model, D=20 μm^2/s, k_1=0.1/s; extended model, D=20 μm^2/s, k_t=0.1/s, k_1=0.000076/s; (B) simple model, D=20 μm^2/s, k_{on}=0.001/(nM·s), k_{off}=0.021/s, k_1=0.00024/s, initial concentration of R in source and target field R_{init}=10 μM [k_{on}, k_{off} and R_{init} were chosen based on values in the literature (Dowd et al., 1999; Umulis et al., 2009)]; extended model, D=20 μm^2/s, k_{on}=0.001/(nM·s), k_{off}=0.021/s, k_t=0.00024/s, k_1=0.000076/s, R_{init}=10 μM. In all models, production of the mobile morphogen only occurred in the source at a constant rate of v=0.2 pM/s. The source and target field were modeled without the effects of cells and tortuosity. Tortuosity could reduce the values of D that were used in the models, and the clearance rate and off-rate constants would change accordingly.

Box 2. Tortuosity

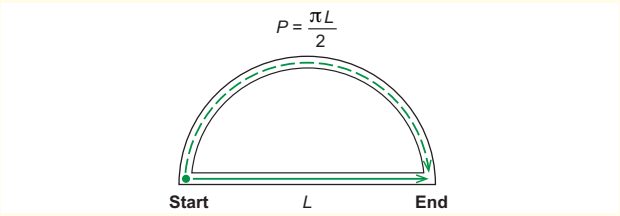

The environment in which a molecule diffuses is said to be 'tortuous' if it contains obstacles that increase the geometric path length of the diffusing molecule. For example, a tissue containing tightly packed cells is more tortuous than one with looser cell packing. The more tortuous the environment, the shorter the average distance that a molecule will travel from its starting point.

To illustrate the effect of tortuosity on diffusion, consider a simple scenario in which a molecule ensemble travels a distance L without obstacles. The average time required to travel distance L is $t=L^2/D_1$ (where D is the diffusion coefficient). Now imagine that a cell is located between the molecule and the destination point at length L away from the initial position (see diagram). In this case, the shortest path (dashed line) would be $P=\pi L/2$. To reach the destination point in the same amount of time in the presence of a cell, $t=L^2/D_1=P^2/D_2=(\pi L/2)^2/D_2$. Thus, the molecules traveling around the cell would need to have a $\pi^2/4\cong2.5$-fold higher diffusion coefficient D_2 than D_1.

mobility. Immobility can be caused by binding to an immobilized diffusion regulator until binding to a mobile diffusion regulator interferes with the former interaction and allows morphogen molecules to move over longer distances. In the drunken sailor analogy, a sailor visits pubs (negative diffusion regulators; Fig. 1E) until a police officer (positive diffusion regulator) escorts the sailor and prevents further pub visits (Fig. 1F). In this analogy, the drunken sailor is largely immobile and can move over longer distances only when escorted by a police officer.

Shuttling is a special case of facilitated diffusion, in which the 'shuttles', not the morphogens, are generated from a localized source (Holley et al., 1996; Eldar et al., 2002; Mizutani et al., 2005; Shimmi et al., 2005; van der Zee et al., 2006; Ben-Zvi et al., 2008; Wang et al., 2008; Ben-Zvi et al., 2011; Haskel-Ittah et al., 2012; Matsuda and Shimmi, 2012; Sawala et al., 2012). The association of morphogen molecules with shuttles results in the formation of a morphogen gradient from an initially broad or even uniform morphogen distribution (Fig. 1E,F). Shuttling involves repeated rounds of: (1) morphogen binding to the shuttle; (2) rapid diffusion of the morphogen-shuttle complex; (3) destruction of the shuttle; and (4) immobilization of the morphogen. When the shuttle molecules are produced at a localized source, morphogens near the source bind shuttle molecules and diffuse away. As morphogen-shuttle complexes diffuse, the shuttles are degraded and morphogen is immobilized. Far from the shuttle source, morphogen molecules accumulate because they are less likely to encounter shuttles and cannot move sufficiently in the absence of shuttles. Eventually, few morphogen molecules are found near the shuttle source but are instead concentrated at a distance. This process generates a sharp gradient from an initially uniform morphogen distribution (Fig. 1E,F).

The facilitated diffusion model has three main predictions. First, in the default state extracellular morphogens are immobilized or significantly hindered in their mobility. Second, competition between the shuttle and the immobilized diffusion regulator releases and mobilizes the morphogen. Third, a localized source of shuttles can generate a morphogen gradient from an initially uniform morphogen distribution.

Transport model 4: transcytosis

As an alternative to extracellular diffusion-based mechanisms (see Box 3 for a discussion of perceived weaknesses of diffusive transport mechanisms), it has been proposed that morphogens are transported via cell-based mechanisms: through cells (transcytosis) or along cellular extensions (cytonemes; see below).

In the transcytosis model, signaling molecules bind to the cell surface, resulting in their cellular uptake by endocytosis. Upon exocytosis the signal is released again from the cell. By undergoing multiple rounds of cellular uptake and release, the molecules become dispersed in the target tissue (Dierick and Bejsovec, 1998; González-Gaitán and Jäckle, 1999; Entchev et al., 2000; Kruse et al., 2004; Bollenbach et al., 2005; Bollenbach et al., 2007; Gallet et al., 2008; Kicheva et al., 2012b). In terms of the drunken sailor analogy, the molecules do not move around the buildings but through the buildings (Fig. 1G). Since the drunken sailors still move by random walks, this process reflects a diffusive behavior, but in contrast to the mechanism discussed earlier it is intracellular.

Box 3. Perceived weaknesses of diffusion-based models

Diffusion-based models of morphogen dispersal have four potential weaknesses concerning (1) the length of patterning fields, (2) the solubility of morphogens, (3) the reliability of patterning and (4) the geometry of patterning fields (Deuchar, 1970; Ramírez-Weber and Kornberg, 2000; Kornberg and Guha, 2007; Wolpert, 2009; Roy and Kornberg, 2011; Kornberg, 2012). First, diffusion cannot generate appropriate gradients sufficiently quickly when the patterning field is large (reviewed by Müller and Schier, 2011). However, the tissues discussed here are all under 500 μm in length, which is small enough that gradients can form by diffusion in time spans (hours to days) consistent with the duration of patterning (Crick, 1970). Second, it has been proposed that the post-translational modifications and hydrophobicity of morphogens prevent their diffusion in aqueous environments. However, multiple mechanisms have been identified that serve to solubilize morphogens (reviewed by Müller and Schier, 2011; Creanga et al., 2012; Haskel-Ittah et al., 2012; Mulligan et al., 2012; Sawala et al., 2012; Tukachinsky et al., 2012). Third, it has been argued that morphogen gradients "*must be constructed with a high degree of reliability; yet it is unlikely that a substance freely diffusible in the extracellular space could provide a very reproducible long-range distribution*" (Kerszberg and Wolpert, 1998). It is clear, however, that precise and robust patterning initiated by morphogen gradients depends on numerous secondary interactions between morphogens, signal transducers, target cells and downstream genes. Thus, secondary interactions can generate highly precise patterns from initially imprecise gradients, and feedback mechanisms can increase the precision of gradients themselves (reviewed by Wartlick et al., 2009; Rogers and Schier, 2011; Kicheva et al., 2012a; Schilling et al., 2012). Fourth, it has been argued that morphogen would be lost from the tissue by diffusion if the tissue geometry were not sufficiently constrained (Kornberg and Guha, 2007; Kornberg, 2012). However, binding interactions can retain the majority of morphogen molecules inside a tissue (Figs 2, 6). Taken together, diffusion-based mechanisms can account for most, if not all, morphogen gradients observed to date, whereas longer-range signaling must rely on mechanisms ranging from cellular extensions to flow-driven transport (reviewed by Müller and Schier, 2011).

The key predictions of the transcytosis model are as follows. First, the morphogen is taken up and released by cells. Second, the effective diffusion coefficient is small because morphogen transport relies on the relatively slow processes of cellular uptake and release. Third, the number of freely moving molecules is expected to be small because most morphogen molecules are bound to transport vehicles at any given point in time. Fourth, gradients can form even when mobile molecules are long-lived because global diffusion is slow. Fifth, gradient shape evolves slowly over time due to slower overall dispersal of the morphogen, similar to the hindered diffusion model.

Transport model 5: cytonemes

As another alternative to extracellular diffusion-based mechanisms, directed delivery mechanisms have been postulated to disperse morphogens (Deuchar, 1970; Miller et al., 1995; Ramírez-Weber and Kornberg, 1999; Ramírez-Weber and Kornberg, 2000; Kerszberg and Wolpert, 2007; Kornberg and Guha, 2007; Wolpert, 2009; Roy and Kornberg, 2011; Kornberg, 2012). One such mechanism is the use of filopodial structures to mediate morphogen transport. There is precedence that such cellular extensions serve to explore the environment, to detect distant signals or to present information to other cells (see Box 4) (Gustafson, 1964; Gustafson and Wolpert, 1967; Karp and Solursh, 1985; Bentley and Toroian-Raymond, 1986; Locke, 1987; Miller et al., 1995; Jacinto et al., 2000; Vasioukhin et al., 2000; Milán et al., 2001; Renaud and Simpson, 2001; Sato and Kornberg, 2002; Wolf et al., 2002; De Joussineau et al., 2003; Rørth, 2003; Gallo and Letourneau, 2004; Yuste and Bonhoeffer, 2004; Lehmann et al., 2005; Demontis and Dahmann, 2007; Kress et al., 2007; Cohen et al., 2010; Swaney et al., 2010; Callejo et al., 2011; Cohen et al., 2011; Inaba et al., 2012; Peng et al., 2012; Rojas-Ríos et al., 2012; Vitriol and Zheng, 2012). The cytoneme model builds on these observations and postulates that long dynamic filopodia-like structures known as cytonemes project from target cells and contact morphogen-producing cells. Morphogens are handed over to and transported along cytonemes to form a concentration gradient (Ramírez-Weber and Kornberg, 1999; Ramírez-Weber and Kornberg, 2000; Sato and Kornberg, 2002; Hsiung et al., 2005; Kornberg and Guha, 2007; Roy and Kornberg, 2011; Kornberg, 2012), akin to drunken sailors taking a subway to their destination (Fig. 1H).

The cytoneme-mediated transport model has four central predictions. First, morphogens do not diffuse extracellularly but are transferred at local contacts between source and target cells. Second, morphogens are transported by cytonemes through the target field. Third, cytonemes extending from target cells orient towards the signaling source over distances that are comparable to the morphogen signaling range. Fourth, because cytonemes must orient towards morphogen sources, morphogen receptors are required for sensing the source and establishing successful contacts.

Box 4. Signal reception and display by filopodia

It is currently unclear whether filopodia function as cytonemes in morphogen transport or gradient formation, but there is precedence for non-cytoneme roles of filopodia in signal reception and display. It is firmly established that filopodial extensions probe gradients of chemoattractants and chemorepellents. For example, developing neurons use filopodial extensions to sense guidance cues and to grow towards synaptic targets (reviewed by Gallo and Letourneau, 2004; Vitriol and Zheng, 2012). Similarly, migratory cells reach their destination by navigating gradients of chemoattractants using cellular extensions (reviewed by Swaney et al., 2010). Filopodia can also sense tissue identity and connect neighboring tissues. For example, *Drosophila* tracheal subunits are connected using FGF-induced cellular extensions (Wolf et al., 2002), and FGF produced in the wing disc attracts tracheal branch filopodia to connect the wing disc to the tracheal system (Sato and Kornberg, 2002). Moreover, during dorsal closure in *Drosophila*, the fusion of two epithelial sheets on the dorsal side is mediated by filopodia that recognize the identity and registration of the opposing tissues (Jacinto et al., 2000). Filopodia also mediate long-range signaling between distant cells. For example, zebrafish stripes are proposed to form via filopodia-mediated interaction between two pigment cell types. Contact results in cell depolarization and repulsion. In the absence of filopodia, the stripes do not form properly (Inaba et al., 2012). Furthermore, filopodia mediate long-range Notch signaling during *Drosophila* bristle formation. Delta and its receptor Notch are both membrane bound, and filopodial extensions allow direct contact between distant cells (Renaud and Simpson, 2001; De Joussineau et al., 2003; Cohen et al., 2010; Cohen et al., 2011). Finally, cellular extensions are used to present signals to target cells. For example, cellular protrusions spatially bias EGF signaling during *Drosophila* mechanosensory organ patterning. EGF-producing source cells send out dynamic protrusions in a biased direction, which is thought to increase the contact and signaling between the producing and the receiving cell (Peng et al., 2012). Similarly, filopodia-like extensions emanating from source cells might present Hedgehog signals to target cells in *Drosophila* (Callejo et al., 2011; Rojas-Ríos et al., 2012).

Experimental analyses of morphogen transport

In recent years, imaging studies and biophysical measurements (see Box 5 and Box 6) have been used to investigate the transport mechanisms of various morphogens, including Nodal, FGF and Dpp, as well as Bicoid (see Box 7). Although these studies have provided some insight into the mechanisms underlying morphogen transport, they have also led to disparate conclusions. For example, several distinct morphogen transport mechanisms have been suggested for gradient formation by Dpp in *Drosophila melanogaster* wing precursors; evidence has been presented for free diffusion, hindered diffusion, transcytosis and cytoneme-mediated transport (Ramírez-Weber and Kornberg, 1999; Hsiung et al., 2005; Kicheva et al., 2007; Roy et al., 2011; Schwank et al., 2011; Wartlick et al., 2011; Zhou et al., 2012). In the following sections, we discuss the experimental evidence that has been put forward to explain the transport of Nodal, FGF and Dpp.

Transport of Nodal morphogens

The Nodal/Lefty morphogen system patterns the germ layers during early embryogenesis over a period of a few hours and the left-right axis during later stages of vertebrate development (reviewed by Schier, 2009). A common theme in these different contexts is that Nodal and its inhibitor Lefty act over different ranges (see Box 8): Nodal activates signaling close to the source, whereas Lefty inhibits Nodal signaling far from the source (Fig. 3A). Recent studies, discussed below, have begun to uncover some of the features of Nodal and Lefty and their modes of transport.

Extracellular localization of Nodal and Lefty

The subcellular localization of morphogens can be an important indicator of what transport process might be at work. For example, if most of the morphogen molecules are found outside cells, it becomes less likely that a concentration gradient is established by movement through cells (e.g. by transcytosis).

Box 5. Measuring transport by FCS

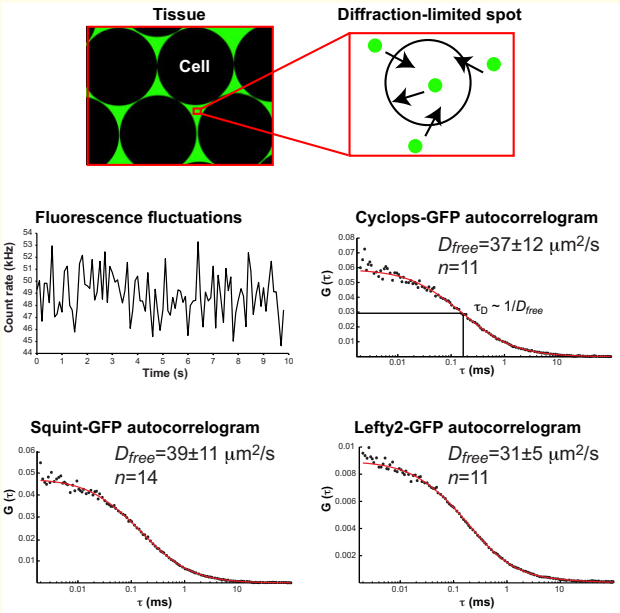

Fluorescence correlation spectroscopy (FCS) analyzes fluorescence fluctuations in small (~femtoliter) volumes (Yu et al., 2009; Griffin et al., 2011; Saunders et al., 2012; Zhou et al., 2012). A laser excites fluorescent molecules in a diffraction-limited and pinhole-confined volume within a tissue. Fluorescence fluctuations are correlated over time and compared with transport model predictions (Ries and Schwille, 2012). FCS thus allows analysis of local transport processes over very short time and length scales. Local extracellular diffusivities of Nodal-GFP and Lefty-GFP were measured in FCS experiments (see figure), similar to those of Yu et al. (Yu et al., 2009). One representative trace of binned fluorescence fluctuations over time is shown. Fluctuations in several of these traces were correlated using different lag times (τ) to calculate the autocorrelation function $G(\tau)$ shown in the autocorrelograms for the zebrafish Nodals Cyclops-GFP and Squint-GFP, as well as for Lefty2-GFP. The diffusion time τ_D is inversely related to the free diffusion coefficient D_{free} and can be found at the inflection point of $G(\tau)$. Pair-correlation function (pCF) microscopy (not shown) is conceptually similar to FCS, but is based on spatial image information, and the fluorescence signal in different areas of an image is correlated and compared with a transport model (Digman and Gratton, 2009; Hinde and Cardarelli, 2011). pCF thus allows analysis of transport processes over longer distances than FCS [e.g. ~500 nm in pCF compared with ~300 nm in FCS (Zhou et al., 2012)].

Nodal and Lefty are members of the transforming growth factor β (TGFβ) superfamily and have signal sequences required for secretion (Zhou et al., 1993; Meno et al., 1996; Beck et al., 2002; Sakuma et al., 2002; Le Good et al., 2005; Jing et al., 2006; Blanchet et al., 2008; Tian et al., 2008; Marjoram and Wright, 2011; Müller et al., 2012). Fusion of the signal sequence-containing N-terminal domains of Nodal and other morphogens to GFP causes secretion of GFP (Entchev et al., 2000; Yu et al., 2009; Müller et al., 2012). Furthermore, western blot analyses reveal efficient secretion of ectopic Nodal-GFP and Lefty-GFP into the extracellular space in zebrafish embryos, and *in vivo* imaging shows extracellular localization of Nodal-GFP and Lefty-GFP (Müller et al., 2012). These results support the idea that Nodal and Lefty are secreted and mainly extracellular.

Tortuosity in the Nodal/Lefty morphogenetic field

The finding that Nodal and Lefty are predominantly extracellular suggests that they move around cells. As discussed above, cells can act as obstacles that increase the path length of molecules diffusing in the extracellular space (see Box 2). As a result, the global effective diffusion coefficient of a population of molecules moving through a tissue should be lower than the local diffusivity within a small extracellular volume. This idea can be tested by studying the movement of secreted GFP using techniques that compare local diffusivity with global effective diffusivity. As described in Box 5 and Box 6, fluorescence correlation spectroscopy (FCS) and fluorescence recovery after photobleaching (FRAP) can measure local and global diffusivity, respectively. FCS experiments for secreted GFP in zebrafish embryos yielded a local extracellular diffusion coefficient of ~90 μm²/s, which is about double the effective diffusion coefficient of ~40 μm²/s measured by FRAP (Yu et al., 2009; Müller et al., 2012). This is consistent with the 50-70% tortuosity-dependent reduction in diffusivity predicted by porous media theory (Nicholson and Syková, 1998; Rusakov and Kullmann, 1998; Nicholson, 2001; Tao and Nicholson, 2004) and observed in densely packed tissues (Thorne and Nicholson, 2006). These results suggest that the tissue architecture of zebrafish embryos can hinder the movement of extracellular morphogens. Interestingly, similar to secreted GFP, FCS and FRAP experiments showed that the local diffusivity of Lefty-GFP (~40 μm²/s) is only about twice its effective diffusivity (~20 μm²/s) (Table 1). These results suggest that the diffusion of secreted GFP and Lefty-GFP is mostly hindered by cell packing but not by binding to extracellular diffusion regulators.

Evidence for hindered diffusion of Nodal

Strikingly, Nodal-GFP has a similar local diffusivity to Lefty-GFP (~40 μm²/s) but a ~90% lower effective diffusivity (~2 μm²/s; Table 1) (Müller et al., 2012). Since secreted GFP, Nodal-GFP and Lefty-GFP move in the same tissue and experience the same tortuosity, additional factors must further decrease the effective diffusivity of Nodal-GFP.

One possibility is that Nodal might transiently bind to immobilized extracellular diffusion regulators (Fig. 3B), which would decrease its effective diffusivity (Crank, 1979; Dowd et al., 1999; Miura et al., 2009; Müller et al., 2012), whereas Lefty does not bind to such regulators and thus moves relatively freely through the tissue (Fig. 3C). The hindered diffusion of Nodal morphogens is not only supported by the low effective diffusion coefficient of Nodal, but also by several additional observations. First, measurements of the extracellular clearance of fluorescent Nodal in zebrafish embryos show a long extracellular half-life of ~100 minutes (Müller et al., 2012), inconsistent with the short half-lives predicted by some forms of the free diffusion model (assuming that extracellular clearance represents clearance of the mobile fraction). Second, nested FRAP experiments (see Box 6) support the hindered diffusion model for Nodal transport. These experiments compare the recovery of fluorescence after photobleaching in two windows: one that encompasses the entire bleached domain, and a smaller one nested within the bleached domain. As predicted by hindered diffusion models, recovery of Nodal-GFP in the smaller window is delayed compared with the large window (Müller et al., 2012). This result is inconsistent with free diffusion models, which predict a very small, experimentally undetectable delay in nested FRAP experiments. Third, the shape of the Nodal gradient is consistent with the measured clearance rate and effective diffusion coefficient and supports the hindered diffusion model (Müller et

Box 6. Measuring transport by FRAP and FSAP

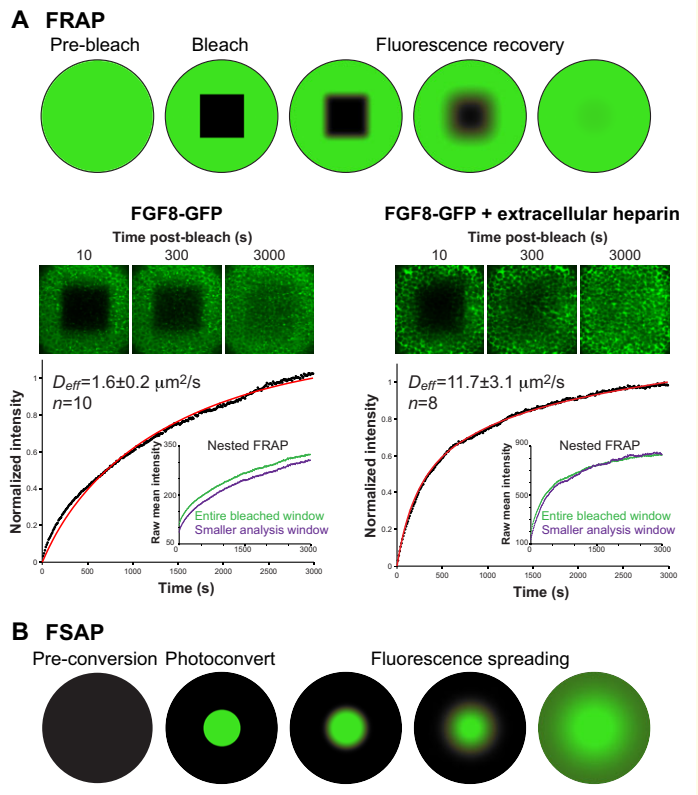

Fluorescence recovery after photobleaching (FRAP) involves photobleaching an area in a fluorescent field and monitoring fluorescence recovery in this area (Lippincott-Schwartz et al., 2003). FRAP can be used to test transport models on different spatial and temporal scales and to determine which factors (e.g. diffusion, production, convection, degradation, binding interactions) influence recovery. Nested FRAP compares fluorescence recovery in the entire bleached area with recovery in a window nested within the bleached area and can determine if recovery is due mainly to diffusion (Sprague and McNally, 2005; Kicheva et al., 2007; Müller et al., 2012; Zhou et al., 2012). FRAP experiments similar to those of Müller et al. (Müller et al., 2012) were performed in zebrafish embryos expressing FGF8-GFP in the presence or absence of exogenous extracellular heparin (A). Nested FRAP in the absence of heparin demonstrates a recovery delay in the nested window, suggesting diffusion-mediated recovery. The delay is not observed in the presence of heparin, probably owing to faster recovery kinetics reflected in the higher effective diffusivity (D_{eff}).

Fluorescence spreading after photoconversion (FSAP) (B) is an experimental mirror image of FRAP (Lippincott-Schwartz et al., 2003; Griffin et al., 2011; Zhou et al., 2012). Molecules tagged with photoconvertible proteins are photoconverted in a localized area and changes in fluorescence are monitored over time, which provides information about molecule movement or clearance (Drocco et al., 2011; Müller et al., 2012). For example, diffusion out of the photoconverted region would result in an increase in intensity outside of the region.

al., 2012). Given the slow clearance and fast local diffusivity of Nodal, gradients formed by free diffusion would be too flat to account for the observed gradient.

The endogenous Nodal gradient has not yet been analyzed, and the identity of potential extracellular Nodal diffusion regulators is currently unknown, but all available data support the predictions from the hindered diffusion model: extracellular morphogen location, high local mobility, low global effective mobility, slow clearance of mobile proteins, a recovery delay in nested FRAP experiments, and a gradient shape consistent with these biophysical measurements.

Transport of FGF morphogens

FGFs are signals with diverse roles in development and homeostasis. Recent biophysical measurements in living zebrafish embryos (Yu et al., 2009; Nowak et al., 2011) and in cultured mammary fibroblasts (Duchesne et al., 2012) have provided insights into the movement of FGFs (FGF2 and FGF8 in particular) from the nano- to the microscopic scale and together support the model of hindered diffusion for FGF morphogen transport.

Evidence for hindered diffusion of FGF8

FGF8 patterns the dorsal-ventral and animal-vegetal axes during zebrafish embryogenesis over a period of a few hours. FGF8 is produced at a localized source and is thought to form a gradient by diffusion and endocytosis-mediated clearance (Scholpp and Brand, 2004; Yu et al., 2009). Fluorescently labeled FGF8 molecules have a local extracellular diffusion coefficient of ~50-80 $\mu m^2/s$ as determined by FCS (Table 1) (Yu et al., 2009; Nowak et al., 2011) but an effective diffusion coefficient of ~2 $\mu m^2/s$ as measured in FRAP experiments (see Box 6). Thus, just like Nodal, FGF8 has a high local diffusivity but a low global effective diffusivity, consistent with the predictions of hindered diffusion models.

The evolution of the extracellular FGF8 gradient provides additional support for hindered diffusion. The gradient shape slowly emerges over time and approaches steady state only after 3 to 4 hours (Fig. 4A) (Yu et al., 2009). The slow emergence of gradient shape is consistent with the hindered diffusion model (Fig. 4B) but not with the free diffusion model (Fig. 4C).

HSPGs as diffusion regulators

What might hinder the movement of FGFs? Heparan sulfate proteoglycans (HSPGs) are excellent candidate diffusion regulators. FGFs are known to interact with the long sugar chains attached to HSPG core proteins (Dowd et al., 1999; Makarenkova et al., 2009; Miura et al., 2009). Disrupting the interactions between HSPGs and FGF2, for example, leads to a dramatically increased FGF2 diffusion coefficient, suggesting that HSPGs might act as negative regulators of FGF2 diffusion (Dowd et al., 1999). Indeed, mathematical modeling of hindered diffusion with fast reversible binding kinetics reproduces experimental observations of FGF2 movement (Dowd et al., 1999).

Recent single-particle tracking approaches have provided a more detailed view of how HSPGs affect the movement of FGF2 (Duchesne et al., 2012). FGF2 molecules cluster in an HSPG-dependent manner in the extracellular matrix. FGF2 spends most of its time in confined motion bound to HSPG-dependent clusters, but FGF2 molecules are not permanently trapped and can diffuse after leaving a cluster. These results support a central tenet of the hindered diffusion model: at any given time the majority of morphogen molecules is reversibly bound to diffusion regulators.

Box 7. Bicoid morphogen

Whereas other morphogens act as extracellular signals in cellularized tissues, Bicoid is a transcription factor that acts in a syncytium. Bicoid patterns the anterior-posterior axis of *Drosophila* embryos. Maternal *bicoid* mRNA is deposited at the anterior, leading to a protein gradient along the anterior-posterior axis (Driever and Nüsslein-Volhard, 1988a; Driever and Nüsslein-Volhard, 1988b; Spirov et al., 2009; Porcher and Dostatni, 2010; Little et al., 2011; Liu and Niranjan, 2011). Measurements of Bicoid-GFP diffusivity in the cytoplasm by FRAP yielded an effective diffusivity of 0.3 $\mu m^2/s$ at mitotic cycle 14 (Gregor et al., 2007). By contrast, FCS determined a local cytoplasmic diffusivity of 7 $\mu m^2/s$ in the cytoplasm and detected two populations of Bicoid-GFP with nuclear diffusivities of 0.2 $\mu m^2/s$ and 8 $\mu m^2/s$ (Abu-Arish et al., 2010; Porcher et al., 2010). Modeling indicates that a diffusivity of 0.3 $\mu m^2/s$ is too low to account for gradient formation by diffusion (Gregor et al., 2007). However, diffusivities were measured after the Bicoid gradient is established, and Bicoid might have a higher diffusivity at earlier times. In addition, a recent reassessment of the FRAP experiments that took into account inhomogeneities arising during photobleaching suggests that the effective Bicoid diffusivity might be ~1 $\mu m^2/s$, which is fast enough to account for gradient formation (Castle et al., 2011). It has recently been proposed that dynamic membrane invaginations within the syncytial embryo could create tortuous paths that lead to anomalous diffusion of Bicoid at short time scales and to a lowering of the effective diffusivity on longer time scales (Daniels et al., 2012). An effect of membrane invaginations on the diffusivity of Bicoid or other molecules has not been measured, but the short invaginations that exist during early embryogenesis might allow Bicoid to diffuse rapidly enough to account for gradient formation.

A role for HSPGs as diffusion regulators is also supported by *in vivo* studies of FGF8 in zebrafish, although single molecule imaging has not yet been achieved in this context. First, a higher fraction of FGF8-GFP is mobile when HSPG sugar chains are destroyed by injection of heparinase I into the extracellular space (Yu et al., 2009). Second, FGF8-GFP has a higher effective diffusion coefficient in embryos injected extracellularly with heparin, which is thought to compete with endogenous HSPGs for FGF8 binding (Fig. 4D). Third, the largely membrane-localized FGF8-GFP signal becomes more diffuse in the extracellular space upon heparin injection, suggesting that this treatment interrupts interactions with diffusion regulators that retain FGF8-GFP at the cell surface (Fig. 4D).

In summary, recent studies of FGF2 and FGF8 transport suggest the following scenario for hindered diffusion. FGF is secreted from source cells but rapidly binds to HSPGs on the cell surface and in the extracellular matrix. FGF molecules are released from HSPGs after a certain residence time and either diffuse and bind to another HSPG molecule or move away from the cell surface to diffuse freely. In this scenario, most of the FGF molecules are bound to HSPGs and are therefore concentrated at the cell surface, whereas a smaller fraction of freely mobile FGF molecules is found far from cell surfaces. Thus, the diffusion of the morphogen punctuated by binding to HSPGs accounts for the formation of the FGF gradient.

Transport of Dpp morphogen

Dpp is a secreted TGFβ superfamily member and a homolog of vertebrate bone morphogenetic proteins (BMPs) (Panganiban et al., 1990a; Panganiban et al., 1990b; Lecuit et al., 1996; Nellen et al., 1996; Lecuit and Cohen, 1998; Entchev et al., 2000; Teleman and Cohen, 2000; Gibson et al., 2002; Belenkaya et al., 2004; Kruse et al., 2004; Kicheva et al., 2007; Schwank et al., 2011; Zhou et al., 2012). A Dpp gradient forms from a localized source and patterns the wing imaginal disc [an epithelial wing precursor tissue that is initially flat and later develops a slight curvature and multiple folds (Sui et al., 2012)] over several days during the larval stages of *Drosophila* development (Entchev et al., 2000; Teleman and Cohen, 2000). Movement of fluorescently labeled Dpp has been directly observed in explanted *Drosophila* wing discs, and multiple transport models have been proposed to explain Dpp gradient formation. Here, we discuss whether Dpp in the wing disc disperses by free or hindered diffusion, by transcytosis, or by cytoneme-mediated transport. We also discuss evidence that Dpp moves by facilitated diffusion during early embryogenesis.

Localization of Dpp

Dpp is present intracellularly and extracellularly, but the relative levels in different locations are under debate (Entchev et al., 2000; Teleman and Cohen, 2000; Belenkaya et al., 2004; Schwank et al.,

Box 8. Signaling range

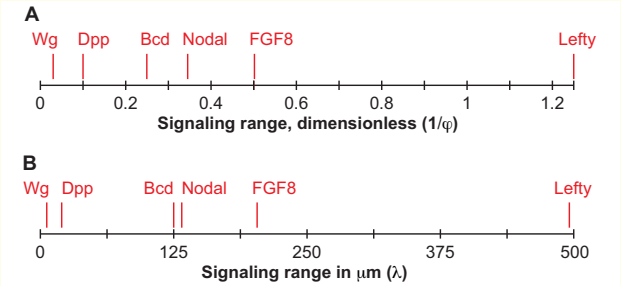

The range over which morphogens induce expression of target genes varies substantially. The morphogens Dpp and Wingless (Wg) have relatively short ranges in the *Drosophila* wing disc (Entchev et al., 2000; Teleman and Cohen, 2000; Kicheva et al., 2007; Bollenbach et al., 2008), Bicoid (Bcd) has a mid-range in *Drosophila* embryos (Driever and Nüsslein-Volhard, 1988a; Driever and Nüsslein-Volhard, 1988b; Gregor et al., 2007; Abu-Arish et al., 2010; Porcher et al., 2010; Castle et al., 2011; Drocco et al., 2011), and Nodal and FGF8 can act over longer distances in zebrafish embryos (Gritsman et al., 2000; Chen and Schier, 2001; Harvey and Smith, 2009; Yu et al., 2009; Müller et al., 2012). Intriguingly, Lefty has a much longer range than Nodal, even though both molecules are TGFβ superfamily members and expressed in zebrafish embryos. The Thiele modulus (a dimensionless number; $\varphi=L\sqrt{k/D}$, where D is the diffusion coefficient, k is the clearance rate constant, and L the length of the field) is a measure of the relative range of a signaling molecule with respect to the length of the patterning field, assuming that the gradient is generated by localized production, diffusion and uniform clearance (Thiele, 1939; Goentoro et al., 2006; Reeves and Stathopoulos, 2009; Haskel-Ittah et al., 2012). The Thiele modulus thus defines the term 'gradient range' and allows for comparison of ranges in differently sized patterning fields (e.g. ranging from 200 μm in the *Drosophila* wing disc to 500 μm in early *Drosophila* embryos). For simplicity, the inverse $1/\varphi$ is shown in A. Low values indicate a short range, whereas large values indicate a long range. For comparison, the absolute range $\lambda=\sqrt{D/k}$ is shown in B. λ and $1/\varphi$ were calculated from literature values of D and k (Gregor et al., 2007; Kicheva et al., 2007; Yu et al., 2009; Abu-Arish et al., 2010; Porcher et al., 2010; Castle et al., 2011; Drocco et al., 2011; Wartlick et al., 2011; Müller et al., 2012; Zhou et al., 2012).

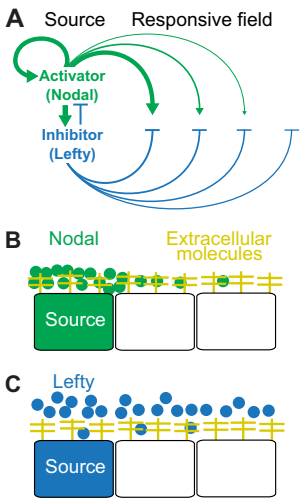

Fig. 3. Model of Nodal and Lefty transport by hindered diffusion. (**A**) Nodal (green) and Lefty (blue) have different signaling ranges and form an activator-inhibitor reaction-diffusion system [modified with permission (Müller et al., 2012)]. Nodal induces signaling at short range due to its low diffusivity, whereas Lefty inhibits Nodal signaling at long range due to its high diffusivity. (**B**,**C**) Mathematical modeling indicates that Nodal (B) might bind to extracellular molecules (yellow) with higher affinity than Lefty (C). This would lead to the decreased global diffusivity of Nodal, whereas Lefty moves relatively freely through the tissue (Müller et al., 2012).

2011). Several lines of evidence suggest that Dpp is largely extracellular. For example, incubation of intact wing discs with proteinase K leads to the digestion of most of the mature Dpp-GFP (Teleman and Cohen, 2000). This suggests that Dpp is accessible extracellularly, although it could be argued that proteinase K might be internalized by endocytosis and thus might also degrade intracellular Dpp. Additional support for extracellular localization comes from incubation of *dpp-GFP*-expressing wing discs with anti-GFP antibodies, resulting in extensive extracellular labeling of Dpp-GFP (Belenkaya et al., 2004; Kruse et al., 2004; Schwank et al., 2011). Although these experiments are consistent with extracellular localization of Dpp-GFP, they do not indicate whether this fraction of Dpp is mobile, as required in extracellular diffusion models. Conversely, it is unclear whether intracellular Dpp is released, as required in transcytosis models, or if Dpp is transferred to and transported by cellular extensions, as proposed in the cytoneme model.

Experimental evidence for Dpp diffusion

FCS and pair-correlation function (pCF) microscopy analyses (see Box 5) indicate that a fraction of fluorescently labeled Dpp moves with a local diffusion coefficient of ~20 μm^2/s in the extracellular space (Zhou et al., 2012). These measurements support extracellular diffusion models, but do not distinguish between free and hindered diffusion. Similarly, currently available data on the kinetics of gradient formation (Entchev et al., 2000; Teleman and Cohen, 2000) cannot distinguish between free and hindered diffusion mechanisms (Fig. 5A-C).

As discussed above, a key prediction of the free diffusion model is rapid morphogen clearance: in order to form a gradient, freely diffusing Dpp would have to be cleared rapidly from the mobile pool, with a half-life of less than 15 seconds (Zhou et al., 2012). The clearance rate of Dpp has not been measured experimentally (Kicheva et al., 2012b), but such low half-lives could result from rapid and irreversible binding to receptors or other immobilized extracellular molecules (Lander et al., 2002). Alternatively, high rates of cellular uptake could rapidly clear Dpp, but this scenario is somewhat less likely as ligand internalization in other systems can take several minutes (Lander et al., 2002).

As a consequence of rapid clearance, only a very small fraction of Dpp-GFP would be mobile extracellularly (Fig. 2A). Consistent with this idea, pulse-labeled Dpp was not observed to move in fluorescence spreading after photoconversion (FSAP) experiments (see Box 6; Fig. 5D) (Zhou et al., 2012). The FSAP experiments support the free diffusion model for Dpp transport, but they are also consistent with the hindered diffusion model when trapping by cellular uptake or permanent immobilization is taken into account (see Fig. 5D-F for details).

The key prediction of the hindered diffusion model is that global diffusivity should be significantly decreased by tortuosity and transient binding. Based on FRAP experiments, Dpp-GFP has been suggested to have a low global effective diffusivity of ~0.1 μm^2/s in the wing disc (Table 1) (Kicheva et al., 2007). A ~95% lower effective diffusion coefficient (Wartlick et al., 2011) was proposed in the smaller haltere imaginal disc (a precursor of a small wing-like organ required for balancing), possibly owing to a higher concentration of diffusion regulators in this tissue (Crickmore and Mann, 2006; de Navas et al., 2006; Crickmore and Mann, 2007; Makhijani et al., 2007). However, these conclusions have been questioned by recent experiments (Zhou et al., 2012) that suggest that the kinetics of Dpp-GFP fluorescence recovery are dominated not by diffusion but by the rates of trapping and degradation of the low levels of highly mobile Dpp (Fig. 5G).

Table 1. Global effective and local free diffusion coefficients

Protein class	Protein	Effective *D* (μm^2/s)	*n*	Free *D* (μm^2/s)	*n*
Nodal	Cyclops-GFP	0.7±0.2*	22	37±12‡	11
	Squint-GFP	3.2±0.5*	30	39±11‡	14
Lefty	Lefty2-GFP	18.9±3.0*	11	31±5‡	11
FGF8	FGF8-GFP	1.6±0.2§	10	53±8¶	29
Dpp	Dpp-GFP	0.1±0.05$^#$	8	10±1**	4
	Dpp-Dendra2	n.d.	n.d.	21±3**	11

n, number of embryos analyzed. Mean diffusion coefficients and standard deviation (*,** standard error) are shown. n.d., not determined.
*FRAP measurements reported by Müller et al. (Müller et al., 2012).
‡FCS measurements similar to those of Yu et al. (Yu et al., 2009) with constructs used by Müller et al. (Müller et al., 2012). Three measurements were taken per embryo. Data were fitted with a one-component model.
§FRAP measurements similar to those of Müller et al. (Müller et al., 2012) with constructs used by Yu et al. (Yu et al., 2009).
¶FCS measurements reported by Yu et al. (Yu et al., 2009).
$^#$FRAP measurements reported by Kicheva et al. (Kicheva et al., 2007).
**FCS measurements reported by Zhou et al. (Zhou et al., 2012).

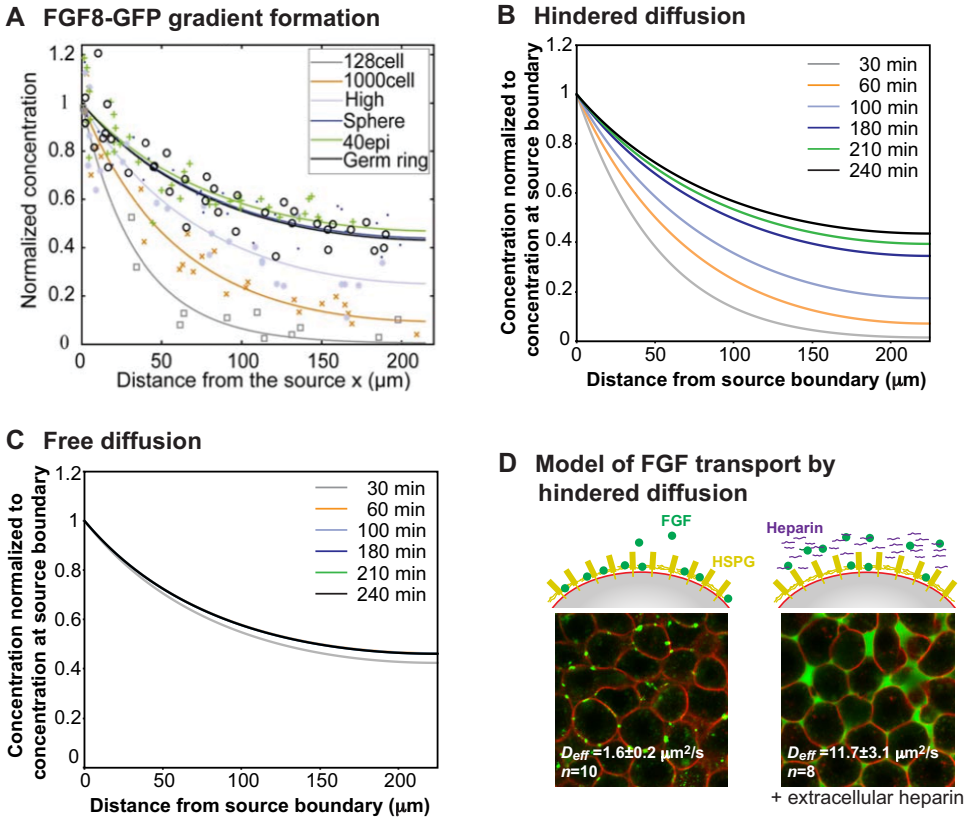

Fig. 4. FGF8 gradient formation dynamics and the hindered diffusion model. (**A**) FGF8-GFP gradient formation dynamics [reproduced with permission (Yu et al., 2009)]. Different colors indicate different developmental stages. In B and C, simulation times were chosen to roughly correspond to the developmental stages measured in A. (**B**) The hindered diffusion model predicts that the gradient emerges slowly over time and qualitatively describes gradient formation similar to that observed *in vivo*. (**C**) By contrast, the free diffusion model predicts that the gradient rapidly (within the first 30 minutes) reaches values close to the steady state distribution. Simulations were performed similar to those of Müller et al. (Müller et al., 2012) using a two-dimensional geometry similar to the geometry described by Yu et al. (Yu et al., 2009). The embryo was modeled as a disc of radius 310 μm containing a concentric source of radius 85 μm, where morphogen is produced at a constant rate; diffusion and reactions occurred in all domains. The equations for the free and hindered diffusion models without trapping shown in Fig. 2 were used. Parameters used: (B) D=50 μm^2/s, k_{on}=0.001/(nM·s), k_{off}=0.065/s, k_1=0.00001/s, R_{init}=1 μM; (C) D=50 μm^2/s, k_1=0.0013/s. Production of the mobile morphogen only occurred in the source at a constant rate of v=0.2 pM/s in all models. Given the homogenous distribution of the binding partner R in this geometry (in contrast to the simulations in Figs 2 and 5, which assume an absence of R in the fluid-filled space), the effective global diffusion coefficient D_{eff} can be calculated from the local free diffusion coefficient D and the binding kinetics as:

$$D_{eff} = \frac{D}{\frac{k_{on} R}{k_{off}} + 1} = 3\,\mu m^2/s \text{ (Crank, 1979; Miura et al., 2009; Müller et al., 2012)}.$$

Source and target field were modeled without the effects of cells and tortuosity. (**D**) Model for FGF transport by hindered diffusion and the effects of heparin injection on FGF8-GFP localization. FGF8-GFP (green) is seen on the cell surface of early zebrafish embryos (left panel; membranes are labeled with membrane-RFP, red). These clusters can be disrupted by injection of 500 pg heparin into the extracellular space at blastula stages (right). The diffuse FGF8-GFP pool in heparin-injected embryos has a dramatically increased diffusion coefficient, suggesting that transient binding to HSPGs might hinder diffusion.

Whether the slow recovery kinetics of Dpp-GFP are due to hindered diffusion or free diffusion can be distinguished in nested FRAP experiments (Fig. 5G; see Box 6). In the free diffusion model, low levels of mobile molecules would rapidly move into the bleached window and fill it almost uniformly. Trapping of mobile molecules would lead to homogeneous changes in fluorescence increases in the bleached window along the gradient over time. By contrast, hindered diffusion predicts that mobile molecules move slowly into the bleached window, causing fluorescence recovery in the outer window prior to the inner window. Thus, hindered diffusion predicts a delay in recovery in the inner window, whereas free diffusion predicts that the recovery in both windows should be experimentally indistinguishable at early times. Such experiments would distinguish between hindered and free diffusion models, but, surprisingly, different groups have obtained conflicting results from nested FRAP experiments (Kicheva et al., 2007; Zhou et al., 2012).

Similar to the hindered diffusion model of FGF transport discussed above, transient binding of Dpp to HSPGs might slow the diffusion of Dpp (Panganiban et al., 1990a; Fujise et al., 2003; Belenkaya et al., 2004; Han et al., 2004; Takei et al., 2004; Akiyama et al., 2008; Dejima et al., 2011). Reduced levels of Dpp are observed in HSPG-deficient tissues (Fujise et al., 2003; Belenkaya et al., 2004; Han et al., 2004; Takei et al., 2004; Akiyama et al., 2008), and increased levels of HSPGs in the source

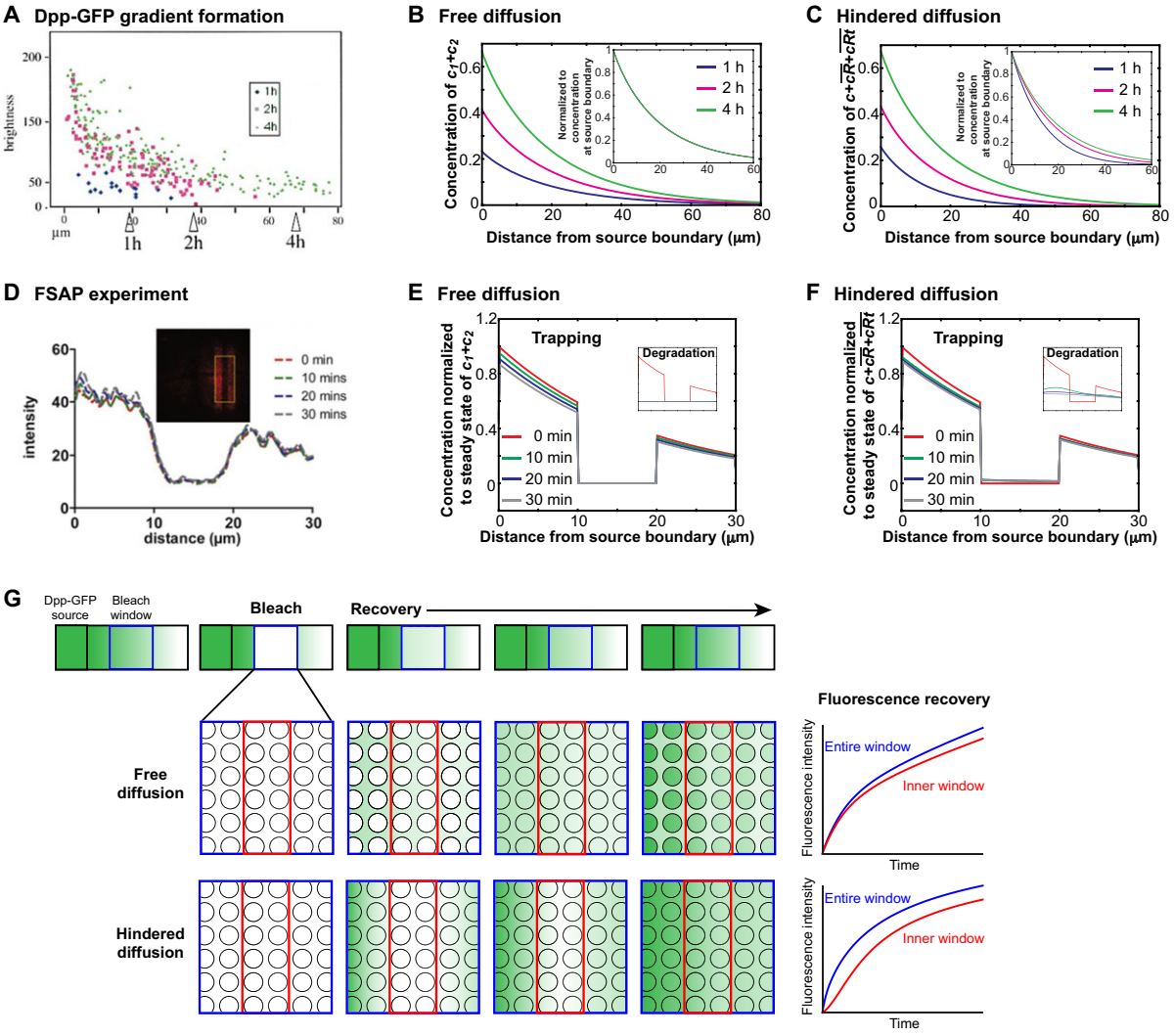

Fig. 5. Dpp gradient formation. (**A**) Dpp-GFP gradient formation dynamics [reproduced with permission (Entchev et al., 2000)]. (**B**,**C**) Gradient formation dynamics predicted by hindered and free diffusion models with trapping in the geometry shown in Fig. 2. Both models appear to fit the data well. Insets show evolution of gradient shape similar to Fig. 2C, normalized to the steady state concentration at the source boundary. Parameters used: (B) D=20 μm^2/s, k_{in}=0.1/s, k_1=0.000076/s; (C) D=20 μm^2/s, k_{on}=0.001/(nM·s), k_{off}=0.021/s, k_{in}=0.00024/s, k_1=0.000076/s, R_{init}=10 μM. Production of mobile morphogen only occurred in the source at a constant rate of v=0.2 pM/s in all models. (**D**) Dpp FSAP [reproduced with permission (Zhou et al., 2012)]. Two parallel stripes in wing discs expressing Dpp-Dendra2 were photoconverted (red), and the photoconverted signal fails to spread. Surprisingly, the fluorescence from pulse-labeled Dpp in FSAP experiments increased, rather than decreased, over time (not shown) (Zhou et al., 2012). (**E**,**F**) FSAP predicted by free (E) and hindered (F) diffusion models with or without clearance by trapping (irreversible binding or cellular uptake) was simulated in a geometry similar to that shown in Fig. 2, except that no new production occurred and that the concentrations of all species were set close to their steady state values in the two photoactivated regions (each 10 μm wide and encompassing both the target field and the fluid-filled space; stripe 1, adjacent to the source boundary; stripe 2, 20 μm away from the source boundary) and to zero everywhere else as the initial condition. Both models that include clearance by trapping appear to fit the data well, and the signal fails to spread due to the long half-life of immobile Dpp combined with the low fraction of mobile molecules. By contrast, the outcomes of models with clearance by degradation (insets) do not resemble the data shown in D. All models with the chosen parameter values led to gradients that attained "*50% of their long-time (100+ hour) values within 8 hours after initiation from initial conditions of zero in all compartments*" and are thus biologically plausible as defined by Zhou et al. (Zhou et al., 2012). Furthermore, similar to experimental results of Kicheva et al. (Kicheva et al., 2007), the system and parameters used in the hindered diffusion models lead to a large 'immobile fraction' and result in a recovery delay between large and small analysis windows in nested FRAP simulations (not shown). Parameters used: free diffusion and no trapping, D=20 μm^2/s, k_1=0.1/s; free diffusion with trapping, D=20 μm^2/s, k_t=0.1/s, k_1=0.000076/s; hindered diffusion with no trapping, D=20 μm^2/s, k_{on}=0.001/(nM·s), k_{off}=0.021/s, k_1=0.00024/s, R_{init}=10 μM; hindered diffusion with trapping, D=20 μm^2/s, k_{on}=0.001/(nM·s), k_{off}=0.021/s, k_t=0.00024/s, k_1=0.000025/s, R_{init}=10 μM. In all models, production of the mobile morphogen only occurred in the source at a constant rate of v=0.2 pM/s. Source and target field were modeled without the effects of cells and tortuosity. (**G**) Schematic of Dpp-GFP nested FRAP (Kicheva et al., 2007; Zhou et al., 2012), comparing fluorescence recovery in a smaller nested window (red) to recovery in the total window (blue). In the free diffusion model, Dpp-GFP quickly diffuses into the bleached region, creating a gradient of low levels of mobile molecules. Over time, permanent trapping in or on cells (circles) results in the accumulation of Dpp-GFP. Because diffusion is fast, no strong recovery delay is predicted; recovery is dominated by binding and degradation kinetics and not by diffusion. By contrast, in the hindered diffusion model, Dpp-GFP moves in from the edge of the bleached window and transiently binds diffusion regulators (not shown), which slows Dpp-GFP and causes fluorescence to recover slowly from the window edge. Here, recovery kinetics are dominated by low effective diffusivity. In both models, the average intensity in the total window at steady state will be higher than in the nested window, as the large window includes a brighter portion of the gradient.

result in a much steeper Dpp gradient (Fujise et al., 2003). Thus, HSPGs may act as Dpp diffusion regulators that retard Dpp movement through the tissue.

Is Dpp diffusion incompatible with tissue architecture?

It has been argued that "*gradient formation based on passive diffusion is incompatible with the […] geometries of the biological systems that use morphogen gradients to regulate their growth and patterning*" (Roy and Kornberg, 2011) and that diffusion "*is an unlikely mechanism to move morphogens for long distances in the plane of the epithelium if it cannot prevent them from moving even a short distance out of the plane*" (Kornberg and Guha, 2007). In the context of Dpp gradient formation in the *Drosophila* wing disc, this concern implies that Dpp movement must be restricted to the plane of the epithelium and that extracellular diffusion cannot retain Dpp (see Box 3 for other perceived weaknesses of diffusion-based models). Instead, cell-based dispersal mechanisms, such as transcytosis and cytonemes (discussed below), would be needed to restrict Dpp movement to the plane of the epithelium.

The wing disc is an epithelial sheet (the disc proper) that is covered apically by a fluid-filled space, similar to the geometry shown in Fig. 2A. Intuitively, it might seem that as morphogen is secreted and moves away from the source, it would be lost into the fluid-filled space (Kornberg, 2012). This perception is incorrect: binding interactions can prevent morphogen loss and retain the majority of molecules within the plane, even if movement is not restricted to the plane. To use the drunken sailor analogy, sailors can encounter a strip of pubs (epithelium) located near an open field (fluid-filled space; Fig. 6A). The sailors' movement is not restricted to the strip, but sailors linger in pubs and are thus hindered in their movement. As a consequence, most of the sailors are found inside pubs over time rather than in the open field. Analogously, a gradient of sailors can form when there is a local source of sailors (Fig. 6B,C).

This model is supported by simulations showing that the combination of (1) localized morphogen production, (2) diffusion in both the disc proper and the fluid-filled space and (3) binding and clearance in the disc proper results in the formation of a morphogen gradient within the plane of the disc proper (Fig. 2A,B). A low-level gradient also forms in the fluid-filled space due to the 'absorptive' effect of binding in the disc proper. Far away from the disc proper, morphogen molecules are almost uniformly distributed, but the distributions in the fluid-filled space are largely irrelevant because morphogen concentrations are very low and morphogen receptors are only present in the disc proper. Importantly, the majority of molecules is bound to the disc proper in a graded fashion. Thus, long-range gradients in the plane of an epithelium can form by diffusion despite unrestricted movement both within and outside of the plane.

Experimental evidence for transcytosis of Dpp

Transcytosis has been suggested as a transport mechanism for Dpp and several other morphogens (Dierick and Bejsovec, 1998; Entchev et al., 2000; Kruse et al., 2004; Bollenbach et al., 2007; Gallet et al., 2008). Specific evidence in support of transcytosis comes from experiments that interfere with endocytosis and the Dpp receptor Tkv: Dpp-GFP accumulates extracellularly around clones lacking Tkv, and clones that cannot perform endocytosis exhibit transiently decreased levels of Dpp within and behind the clones (Entchev et al., 2000). Furthermore, global but transient inhibition of endocytosis can prevent observable Dpp-GFP spreading, which is rescued when endocytosis is restored (Kicheva et al., 2007). These findings support the idea that receptor-mediated endocytosis is necessary for Dpp movement. However, this conclusion has been undermined by the suggestion that *tkv* mutant clones are likely to be abnormal (Schwank et al., 2011). Indeed, *tkv* mutant clones are normally eliminated due to the activity of the transcription factor Brinker, and Dpp can move through receptor-free regions that are mutant for both *tkv* and *brinker* (Schwank et al., 2011). These results suggest that receptor-mediated endocytosis does not play a role in Dpp movement. It is still conceivable, however, that receptor-independent modes of internalization (e.g. fluid phase uptake or internalization stimulated by an alternative membrane-bound binding partner) mediate transcytosis.

Additional evidence against transcytosis is the lack of detectable spreading of Dpp during the FSAP experiments described above (Zhou et al., 2012) (Fig. 5D), despite the postulation that a significant fraction of intracellular Dpp should move during transcytosis. Finally, the key prediction of the transcytosis model, i.e. repeated cellular uptake and release, has not been observed for any morphogen.

Experimental evidence for cytoneme-mediated transport of Dpp

It is well established that filopodia-like processes can mediate signaling between distant cells (see Box 4), but it has been suggested that these structures are also required for morphogen transport and gradient formation. For example, filopodia in cultured

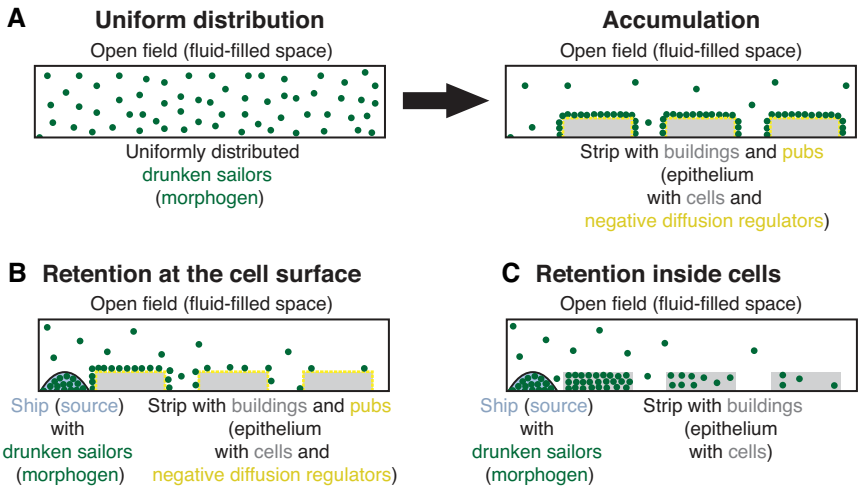

Fig. 6. Retention of diffusing morphogen molecules in the plane of the target tissue. (**A**) Binding interactions can retain the majority of morphogen molecules within the plane of an epithelium, even if movement is not restricted to the plane. This effect is illustrated using the drunken sailor analogy. When sailors (morphogen, green) encounter a strip of pubs (epithelium, gray) located near an open field (fluid-filled space), sailors associate with pubs (yellow). Even though the sailors' movement is not restricted to the strip, their movement is hindered once inside a pub and most of the sailors are found in pubs over time rather than in the open field. (**B**,**C**) A gradient of sailors can form when there is a local source of sailors. Retention of morphogen molecules in the plane of the epithelium could be caused by binding to the cell surface (B) or by cellular uptake (C).

mammalian cells can transport signals to the cell body (Lidke et al., 2004; Lidke et al., 2005). Filopodia-like extensions called cytonemes emanate from target cells in the *Drosophila* wing disc and project to the Dpp source (Ramírez-Weber and Kornberg, 1999; Hsiung et al., 2005; Roy et al., 2011). It has been proposed that Dpp is transferred to and delivered along cytonemes, leading to Dpp gradient formation (Roy et al., 2011). There are clear connections between cytonemes and Dpp signaling: cytoneme formation requires Dpp signaling; ectopic sources of Dpp can orient cytonemes; and vesicles containing Dpp receptors (Tkv) have been observed along the length of cytonemes (Fig. 7). These observations support a role for Dpp in cytoneme formation and polarity, but it is unclear whether cytonemes are involved in Dpp gradient formation. For example, it is not known whether Dpp is associated with and transported by wing disc cytonemes (Hsiung et al., 2005; Demontis and Dahmann, 2007), and there is no evidence that cytonemes are required for Dpp gradient formation.

How might the role of cytonemes in gradient formation be tested? One possibility is to block or reduce cytoneme formation and determine whether a gradient can still form. Such an experiment has become feasible by the observation that uniform Dpp induces stumpy, disoriented cytonemes (Fig. 7B) (Ramírez-Weber and Kornberg, 1999; Hsiung et al., 2005; Roy et al., 2011). If cytonemes are required for gradient formation, uniform expression of unlabeled Dpp should not only block the formation of long cytonemes but also preclude gradient formation (or significantly decrease the gradient length scale) of Dpp-GFP expressed from the endogenous Dpp source (Fig. 7C). This experiment has not yet been performed in *Drosophila*, but in zebrafish embryos Nodal-GFP gradients form properly even when unlabeled Nodal is ubiquitously expressed (Müller et al., 2012).

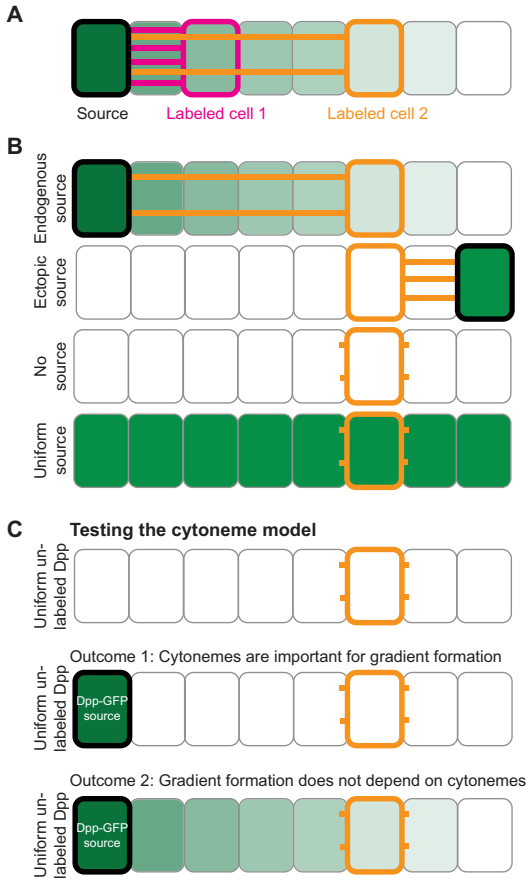

Fig. 7. Cytoneme-mediated morphogen gradient formation. (**A**) In the cytoneme model, cells project filopodia (pink and orange lines) toward the morphogen source (dark green) and transport morphogen from the source to the cell body. It is possible that cells closer to the source have more cytonemes that contact the source than cells farther away and can thereby establish a gradient in the target tissue even if transport rates in the cytonemes are fast. (**B**) Cytonemes extend toward morphogen sources. An ectopic source can compete with the endogenous morphogen source to attract cytonemes. In the absence of a morphogen source or in the presence of a uniform morphogen concentration, cells only develop short, randomly oriented cytonemes (Ramírez-Weber and Kornberg, 1999; Hsiung et al., 2005; Roy et al., 2011). (**C**) Testing the cytoneme model. The cytoneme model predicts that the short, randomly oriented filopodia resulting from uniform expression of unlabeled Dpp should preclude long-range gradient formation of fluorescent Dpp-GFP expressed from a local source (outcome 1). By contrast, if Dpp transport does not depend on cytonemes, the Dpp-GFP gradient should still form when unlabeled Dpp is uniformly expressed (outcome 2).

Shuttling of Dpp in the early *Drosophila* embryo

Dpp patterns not only the larval wing disc, but also the dorsal-ventral axis during early embryogenesis. In this context, *dpp* RNA is expressed dorsolaterally in a broad domain, but Dpp protein forms a sharp gradient that peaks dorsally (Fig. 8A). It is thought that this gradient forms by the shuttling of Dpp molecules towards the dorsal side. In contrast to transport models in which morphogens are expressed from a localized source, shuttling allows the formation of a gradient in the absence of a localized morphogen source.

Dpp movement in the early embryo is hindered by strong binding to cell surface-associated collagen (Wang et al., 2008; Sawala et al., 2012). Dpp can be released from collagen and mobilized by binding to a secreted Short gastrulation (Sog) complex (the shuttle). The Tolloid protease cleaves Sog and releases Dpp from this complex on the dorsal side of the embryo. Dpp is thought to then reassociate with immobile collagen. Because Sog is expressed in a more ventral domain than Dpp, repeated rounds of complex formation, rapid diffusion and Sog cleavage lead to the accumulation of Dpp on the dorsal side of the embryo (Fig. 8A; Fig. 1E,F). Strikingly, Dpp-GFP expressed in a stripe perpendicular to its endogenous expression domain is also redistributed to the dorsal side, strongly supporting the shuttling model (Wang and Ferguson, 2005).

A similar mechanism might act in BMP-Chordin signaling in frogs (Reversade and De Robertis, 2005; Ben-Zvi et al., 2008; Francois et al., 2009). Moreover, a variation on the shuttling theme, in which a localized source of shuttling molecules is generated by self-organization, has recently been described for the Spätzle morphogen system (Haskel-Ittah et al., 2012), which patterns the dorsal-ventral axis in *Drosophila* before the onset of the Dpp patterning system (see Fig. 8B,C for details). Despite the elegance of the shuttling model, direct visualization and biophysical measurements of Dpp/BMP or Spätzle diffusion and shuttling are not yet available (see Box 9 for biophysical evidence for shuttling of other cell fate determinants).

Conclusions and perspectives

The morphogen concept was conceived more than a century ago, and the distribution of a morphogen (Bicoid, see Box 7) within an embryo was first visualized 25 years ago (reviewed by Rogers and Schier, 2011). Over the last ten years, biophysical research has

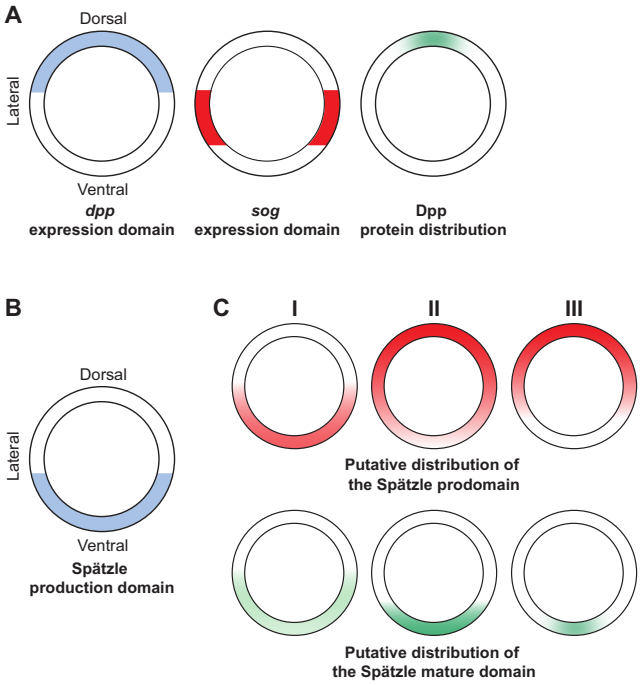

Fig. 8. Transport by facilitated diffusion. (**A**) In early *Drosophila* embryos, *Dpp* is expressed in a broad dorsolateral domain (blue), but the Dpp protein gradient (green) peaks dorsally. The putative Dpp shuttling molecule Sog (red) is expressed ventrolaterally and is thought to concentrate Dpp dorsally using the shuttling mechanism described in Fig. 1E,F. (**B**,**C**) Spätzle patterns the dorsal-ventral axis in *Drosophila* before the onset of the Dpp patterning system. It has recently been proposed that the Spätzle system self-organizes to generate an effective source of shuttling molecules, although the shuttle is produced within the morphogen domain (Haskel-Ittah et al., 2012). (B) Spätzle is produced in a broad ventral domain (blue), but signaling is highest in a narrow ventral stripe (reviewed by Moussian and Roth, 2005). (C) Spätzle is produced as a precursor protein that is cleaved into a mature domain (green) and a prodomain (red). Both are postulated to be produced ventrally initially (I). The mature domain activates signaling, whereas the prodomain inhibits signaling and has been suggested to diffuse more quickly than the mature domain (Morisato, 2001). The prodomain and the mature domain can reassociate (Haskel-Ittah et al., 2012) and, based on mathematical modeling, it has been proposed that the reassociated complex is more diffusive than the mature domain and that the prodomain is quickly degraded when recomplexed, thereby locally depositing the immobile mature domain (Haskel-Ittah et al., 2012). This leads to depletion of the prodomain wherever the mature domain is present and thus creates higher levels of the prodomain outside of the Spätzle production domain (II). The higher levels of prodomain that are generated in lateral domains over time effectively constitute a source of positive diffusion regulators that shuttle the mature domain into a sharp ventral stripe (III) (Haskel-Ittah et al., 2012). Direct biophysical measurements of diffusion and shuttling of Spätzle are currently lacking, and an alternative system that assumes conversion (and thus depletion) of highly diffusive precursor molecules into less mobile signaling activators can also account for many of the patterning properties of the Spätzle system (Meinhardt, 2004).

started to explore the dynamics of morphogen movement and gradient formation to reveal potential modes of morphogen transport. Our analysis of the currently available data leads us to favor diffusion-based models of morphogen transport: morphogens move through tissues by diffusion that is slowed down by tortuosity and hindered (and in some cases facilitated) by transient binding to extracellular molecules.

Box 9. Biophysical evidence for shuttling

Direct biophysical measurements of diffusion and shuttling in the Dpp/BMP and Spätzle morphogen systems are currently lacking. However, biophysical evidence supporting the shuttling model exists for other cell fate determinants that do not act as classical morphogens (Tenlen et al., 2008; Daniels et al., 2009; Daniels et al., 2010; Griffin et al., 2011). For example, a gradient of the cell fate determinant MEX-5 patterns the anterior-posterior axis in *Caenorhabditis elegans* embryos. At the one-cell stage, MEX-5 is initially distributed uniformly throughout the embryo and bound to RNA, which hinders its diffusion ($D \cong 0.07$ μm^2/s) (Griffin et al., 2011). Phosphorylation by the kinase PAR-1 prevents MEX-5 from binding to RNA and therefore increases its diffusivity ($D \cong 5$ μm^2/s). Thus, RNAs act as negative diffusion regulators, whereas PAR-1 acts as a positive diffusion regulator of MEX-5. Shortly after fertilization, the kinase PAR-1 becomes localized in a gradient that peaks on the posterior side of the embryo, whereas a phosphatase that dephosphorylates MEX-5, and thereby allows reassociation with largely immobile RNAs, is uniformly distributed throughout the embryo. Conceptually similar to Dpp and Spätzle shuttling, repeated rounds of RNA binding, phosphorylation, rapid diffusion and dephosphorylation lead to the concentration of MEX-5 on the anterior side (Griffin et al., 2011).

Future research will address the following questions. Does a universal morphogen transport mechanism exist, or do morphogens use unique dispersal strategies depending on developmental context (Kornberg, 2012)? Why do signaling ranges differ widely between morphogens and tissue contexts [including the apical and basal surfaces of the same epithelium (Ayers et al., 2010)]? How is morphogen movement affected by the growth and morphogenesis of target tissues? What factors regulate morphogen movement and signaling range? What does the environment through which morphogens move look like, and how does that environment affect dispersal? What are the nanometer to micrometer scale transport mechanisms that together lead to macroscopic gradient formation (Müller and Schier, 2011)?

Answers to these questions might be found using quantitative imaging and modeling techniques, such as single-plane illumination microscopy FCS (SPIM-FCS) (Sankaran et al., 2010; Wohland et al., 2010; Capoulade et al., 2011), single-particle tracking (Duchesne et al., 2012) and multi-scale modeling approaches (Kavousanakis et al., 2010; Sample and Shvartsman, 2010; Daniels et al., 2012), to analyze transport over different time and length scales (Grimm et al., 2010). Such approaches will help to reveal more clearly how morphogen gradients form during development.

Acknowledgements

We thank Markus Affolter, Konrad Basler, James Briscoe, Edwin Ferguson, James Gagnon, Marcos González-Gaitán, Fisun Hamaratoglu-Dion, Ben Jordan, Thomas Kornberg, Arthur Lander, Andrea Pauli and David Schoppik for helpful comments and discussions.

Funding

This study was supported by the National Institutes of Health, the National Science Foundation, the Human Frontier Science Program, and the Harvard Graduate School of Arts and Sciences. Deposited in PMC for release after 12 months.

Competing interests statement

The authors declare no competing financial interests.

References

Abu-Arish, A., Porcher, A., Czerwonka, A., Dostatni, N. and Fradin, C. (2010). High mobility of bicoid captured by fluorescence correlation spectroscopy: implication for the rapid establishment of its gradient. *Biophys. J.* **99**, L33-L35.

Akiyama, T., Kamimura, K., Firkus, C., Takeo, S., Shimmi, O. and Nakato, H. (2008). Dally regulates Dpp morphogen gradient formation by stabilizing Dpp on the cell surface. *Dev. Biol.* **313**, 408-419.
Ayers, K. L., Gallet, A., Staccini-Lavenant, L. and Thérond, P. P. (2010). The long-range activity of Hedgehog is regulated in the apical extracellular space by the glypican Dally and the hydrolase Notum. *Dev. Cell* **18**, 605-620.
Baeg, G. H., Selva, E. M., Goodman, R. M., Dasgupta, R. and Perrimon, N. (2004). The Wingless morphogen gradient is established by the cooperative action of Frizzled and Heparan Sulfate Proteoglycan receptors. *Dev. Biol.* **276**, 89-100.
Beck, S., Le Good, J. A., Guzman, M., Ben Haim, N., Roy, K., Beermann, F. and Constam, D. B. (2002). Extraembryonic proteases regulate Nodal signalling during gastrulation. *Nat. Cell Biol.* **4**, 981-985.
Belenkaya, T. Y., Han, C., Yan, D., Opoka, R. J., Khodoun, M., Liu, H. and Lin, X. (2004). Drosophila Dpp morphogen movement is independent of dynamin-mediated endocytosis but regulated by the glypican members of heparan sulfate proteoglycans. *Cell* **119**, 231-244.
Ben-Zvi, D., Shilo, B. Z., Fainsod, A. and Barkai, N. (2008). Scaling of the BMP activation gradient in Xenopus embryos. *Nature* **453**, 1205-1211.
Ben-Zvi, D., Pyrowolakis, G., Barkai, N. and Shilo, B. Z. (2011). Expansion-repression mechanism for scaling the Dpp activation gradient in Drosophila wing imaginal discs. *Curr. Biol.* **21**, 1391-1396.
Bentley, D. and Toroian-Raymond, A. (1986). Disoriented pathfinding by pioneer neurone growth cones deprived of filopodia by cytochalasin treatment. *Nature* **323**, 712-715.
Berg, H. C. (1993). *Random Walks in Biology*. Princeton, NJ: Princeton University Press.
Blanchet, M. H., Le Good, J. A., Mesnard, D., Oorschot, V., Baflast, S., Minchiotti, G., Klumperman, J. and Constam, D. B. (2008). Cripto recruits Furin and PACE4 and controls Nodal trafficking during proteolytic maturation. *EMBO J.* **27**, 2580-2591.
Bollenbach, T., Kruse, K., Pantazis, P., González-Gaitán, M. and Jülicher, F. (2005). Robust formation of morphogen gradients. *Phys. Rev. Lett.* **94**, 018103.
Bollenbach, T., Kruse, K., Pantazis, P., González-Gaitán, M. and Jülicher, F. (2007). Morphogen transport in epithelia. *Phys. Rev. E Stat. Nonlin. Soft Matter Phys.* **75**, 011901.
Bollenbach, T., Pantazis, P., Kicheva, A., Bökel, C., González-Gaitán, M. and Jülicher, F. (2008). Precision of the Dpp gradient. *Development* **135**, 1137-1146.
Callejo, A., Torroja, C., Quijada, L. and Guerrero, I. (2006). Hedgehog lipid modifications are required for Hedgehog stabilization in the extracellular matrix. *Development* **133**, 471-483.
Callejo, A., Bilioni, A., Mollica, E., Gorfinkiel, N., Andrés, G., Ibáñez, C., Torroja, C., Doglio, L., Sierra, J. and Guerrero, I. (2011). Dispatched mediates Hedgehog basolateral release to form the long-range morphogenetic gradient in the Drosophila wing disk epithelium. *Proc. Natl. Acad. Sci. USA* **108**, 12591-12598.
Capoulade, J., Wachsmuth, M., Hufnagel, L. and Knop, M. (2011). Quantitative fluorescence imaging of protein diffusion and interaction in living cells. *Nat. Biotechnol.* **29**, 835-839.
Castle, B. T., Howard, S. A. and Odde, D. J. (2011). Assessment of transport mechanisms underlying the nicoid morphogen gradient. *Cell. Mol. Bioeng.* **4**, 116-121.
Chen, Y. and Schier, A. F. (2001). The zebrafish Nodal signal Squint functions as a morphogen. *Nature* **411**, 607-610.
Cohen, M., Georgiou, M., Stevenson, N. L., Miodownik, M. and Baum, B. (2010). Dynamic filopodia transmit intermittent Delta-Notch signaling to drive pattern refinement during lateral inhibition. *Dev. Cell* **19**, 78-89.
Cohen, M., Baum, B. and Miodownik, M. (2011). The importance of structured noise in the generation of self-organizing tissue patterns through contact-mediated cell-cell signalling. *J. R. Soc. Interface* **8**, 787-798.
Crank, J. (1979). *The Mathematics of Diffusion*. Oxford: Clarendon Press.
Creanga, A., Glenn, T. D., Mann, R. K., Saunders, A. M., Talbot, W. S. and Beachy, P. A. (2012). Scube/You activity mediates release of dually lipid-modified Hedgehog signal in soluble form. *Genes Dev.* **26**, 1312-1325.
Crick, F. (1970). Diffusion in embryogenesis. *Nature* **225**, 420-422.
Crickmore, M. A. and Mann, R. S. (2006). Hox control of organ size by regulation of morphogen production and mobility. *Science* **313**, 63-68.
Crickmore, M. A. and Mann, R. S. (2007). Hox control of morphogen mobility and organ development through regulation of glypican expression. *Development* **134**, 327-334.
Daniels, B. R., Perkins, E. M., Dobrowsky, T. M., Sun, S. X. and Wirtz, D. (2009). Asymmetric enrichment of PIE-1 in the Caenorhabditis elegans zygote mediated by binary counterdiffusion. *J. Cell Biol.* **184**, 473-479.
Daniels, B. R., Dobrowsky, T. M., Perkins, E. M., Sun, S. X. and Wirtz, D. (2010). MEX-5 enrichment in the C. elegans early embryo mediated by differential diffusion. *Development* **137**, 2579-2585.
Daniels, B. R., Rikhy, R., Renz, M., Dobrowsky, T. M. and Lippincott-Schwartz, J. (2012). Multiscale diffusion in the mitotic Drosophila melanogaster syncytial blastoderm. *Proc. Natl. Acad. Sci. USA* **109**, 8588-8593.
De Joussineau, C., Soulé, J., Martin, M., Anguille, C., Montcourrier, P. and Alexandre, D. (2003). Delta-promoted filopodia mediate long-range lateral inhibition in Drosophila. *Nature* **426**, 555-559.
de Navas, L. F., Garaulet, D. L. and Sánchez-Herrero, E. (2006). The ultrabithorax Hox gene of Drosophila controls haltere size by regulating the Dpp pathway. *Development* **133**, 4495-4506.
Dejima, K., Kanai, M. I., Akiyama, T., Levings, D. C. and Nakato, H. (2011). Novel contact-dependent bone morphogenetic protein (BMP) signaling mediated by heparan sulfate proteoglycans. *J. Biol. Chem.* **286**, 17103-17111.
Demontis, F. and Dahmann, C. (2007). Apical and lateral cell protrusions interconnect epithelial cells in live Drosophila wing imaginal discs. *Dev. Dyn.* **236**, 3408-3418.
Deuchar, E. M. (1970). Diffusion in embryogenesis. *Nature* **225**, 671.
Dierick, H. A. and Bejsovec, A. (1998). Functional analysis of Wingless reveals a link between intercellular ligand transport and dorsal-cell-specific signaling. *Development* **125**, 4729-4738.
Digman, M. A. and Gratton, E. (2009). Imaging barriers to diffusion by pair correlation functions. *Biophys. J.* **97**, 665-673.
Dowd, C. J., Cooney, C. L. and Nugent, M. A. (1999). Heparan sulfate mediates bFGF transport through basement membrane by diffusion with rapid reversible binding. *J. Biol. Chem.* **274**, 5236-5244.
Driever, W. and Nüsslein-Volhard, C. (1988a). A gradient of bicoid protein in Drosophila embryos. *Cell* **54**, 83-93.
Driever, W. and Nüsslein-Volhard, C. (1988b). The bicoid protein determines position in the Drosophila embryo in a concentration-dependent manner. *Cell* **54**, 95-104.
Drocco, J. A., Grimm, O., Tank, D. W. and Wieschaus, E. (2011). Measurement and perturbation of morphogen lifetime: effects on gradient shape. *Biophys. J.* **101**, 1807-1815.
Duchesne, L., Octeau, V., Bearon, R. N., Beckett, A., Prior, I. A., Lounis, B. and Fernig, D. G. (2012). Transport of fibroblast growth factor 2 in the pericellular matrix is controlled by the spatial distribution of its binding sites in heparan sulfate. *PLoS Biol.* **10**, e1001361.
Eldar, A., Dorfman, R., Weiss, D., Ashe, H., Shilo, B. Z. and Barkai, N. (2002). Robustness of the BMP morphogen gradient in Drosophila embryonic patterning. *Nature* **419**, 304-308.
Entchev, E. V., Schwabedissen, A. and González-Gaitán, M. (2000). Gradient formation of the TGF-β homolog Dpp. *Cell* **103**, 981-991.
Francois, P., Vonica, A., Brivanlou, A. H. and Siggia, E. D. (2009). Scaling of BMP gradients in Xenopus embryos. *Nature* **461**, E1.
Fujise, M., Takeo, S., Kamimura, K., Matsuo, T., Aigaki, T., Izumi, S. and Nakato, H. (2003). Dally regulates Dpp morphogen gradient formation in the Drosophila wing. *Development* **130**, 1515-1522.
Gallet, A., Staccini-Lavenant, L. and Thérond, P. P. (2008). Cellular trafficking of the glypican Dally-like is required for full-strength Hedgehog signaling and wingless transcytosis. *Dev. Cell* **14**, 712-725.
Gallo, G. and Letourneau, P. C. (2004). Regulation of growth cone actin filaments by guidance cues. *J. Neurobiol.* **58**, 92-102.
Gibson, M. C., Lehman, D. A. and Schubiger, G. (2002). Lumenal transmission of decapentaplegic in Drosophila imaginal discs. *Dev. Cell* **3**, 451-460.
Goentoro, L. A., Reeves, G. T., Kowal, C. P., Martinelli, L., Schüpbach, T. and Shvartsman, S. Y. (2006). Quantifying the Gurken morphogen gradient in Drosophila oogenesis. *Dev. Cell* **11**, 263-272.
González-Gaitán, M. and Jäckle, H. (1999). The range of spalt-activating Dpp signalling is reduced in endocytosis-defective Drosophila wing discs. *Mech. Dev.* **87**, 143-151.
Gregor, T., Wieschaus, E. F., McGregor, A. P., Bialek, W. and Tank, D. W. (2007). Stability and nuclear dynamics of the bicoid morphogen gradient. *Cell* **130**, 141-152.
Griffin, E. E., Odde, D. J. and Seydoux, G. (2011). Regulation of the MEX-5 gradient by a spatially segregated kinase/phosphatase cycle. *Cell* **146**, 955-968.
Grimm, O., Coppey, M. and Wieschaus, E. (2010). Modelling the Bicoid gradient. *Development* **137**, 2253-2264.
Gritsman, K., Talbot, W. S. and Schier, A. F. (2000). Nodal signaling patterns the organizer. *Development* **127**, 921-932.
Gustafson, T. (1964). *The Role and Activities of Pseudopodia During Morphogenesis of the Sea Urchin Larva*. Orlando, FL: Academic Press.
Gustafson, T. and Wolpert, L. (1967). Cellular movement and contact in sea urchin morphogenesis. *Biol. Rev. Camb. Philos. Soc.* **42**, 442-498.
Han, C., Belenkaya, T. Y., Khodoun, M., Tauchi, M., Lin, X. and Lin, X. (2004). Distinct and collaborative roles of Drosophila EXT family proteins in morphogen signalling and gradient formation. *Development* **131**, 1563-1575.
Han, C., Yan, D., Belenkaya, T. Y. and Lin, X. (2005). Drosophila glypicans Dally and Dally-like shape the extracellular Wingless morphogen gradient in the wing disc. *Development* **132**, 667-679.
Harvey, S. A. and Smith, J. C. (2009). Visualisation and quantification of morphogen gradient formation in the zebrafish. *PLoS Biol.* **7**, e1000101.

Haskel-Ittah, M., Ben-Zvi, D., Branski-Arieli, M., Schejter, E. D., Shilo, B. Z. and Barkai, N. (2012). Self-organized shuttling: generating sharp dorsoventral polarity in the early Drosophila embryo. *Cell* **150**, 1016-1028.
Hinde, E. and Cardarelli, F. (2011). Measuring the flow of molecules in cells. *Biophys. Rev.* **3**, 119-129.
Holley, S. A., Neul, J. L., Attisano, L., Wrana, J. L., Sasai, Y., O'Connor, M. B., De Robertis, E. M. and Ferguson, E. L. (1996). The Xenopus dorsalizing factor noggin ventralizes Drosophila embryos by preventing DPP from activating its receptor. *Cell* **86**, 607-617.
Hsiung, F., Ramírez-Weber, F. A., Iwaki, D. D. and Kornberg, T. B. (2005). Dependence of Drosophila wing imaginal disc cytonemes on Decapentaplegic. *Nature* **437**, 560-563.
Hufnagel, L., Kreuger, J., Cohen, S. M. and Shraiman, B. I. (2006). On the role of glypicans in the process of morphogen gradient formation. *Dev. Biol.* **300**, 512-522.
Inaba, M., Yamanaka, H. and Kondo, S. (2012). Pigment pattern formation by contact-dependent depolarization. *Science* **335**, 677.
Jacinto, A., Wood, W., Balayo, T., Turmaine, M., Martinez-Arias, A. and Martin, P. (2000). Dynamic actin-based epithelial adhesion and cell matching during Drosophila dorsal closure. *Curr. Biol.* **10**, 1420-1426.
Jing, X. H., Zhou, S. M., Wang, W. Q. and Chen, Y. (2006). Mechanisms underlying long- and short-range nodal signaling in zebrafish. *Mech. Dev.* **123**, 388-394.
Karp, G. C. and Solursh, M. (1985). Dynamic activity of the filopodia of sea urchin embryonic cells and their role in directed migration of the primary mesenchyme in vitro. *Dev. Biol.* **112**, 276-283.
Kavousanakis, M. E., Kanodia, J. S., Kim, Y., Kevrekidis, I. G. and Shvartsman, S. Y. (2010). A compartmental model for the bicoid gradient. *Dev. Biol.* **345**, 12-17.
Kerszberg, M. and Wolpert, L. (1998). Mechanisms for positional signalling by morphogen transport: a theoretical study. *J. Theor. Biol.* **191**, 103-114.
Kerszberg, M. and Wolpert, L. (2007). Specifying positional information in the embryo: looking beyond morphogens. *Cell* **130**, 205-209.
Kicheva, A., Pantazis, P., Bollenbach, T., Kalaidzidis, Y., Bittig, T., Jülicher, F. and González-Gaitán, M. (2007). Kinetics of morphogen gradient formation. *Science* **315**, 521-525.
Kicheva, A., Cohen, M. and Briscoe, J. (2012a). Developmental pattern formation: insights from physics and biology. *Science* **338**, 210-212.
Kicheva, A., Bollenbach, T., Wartlick, O., Jülicher, F. and González-Gaitan, M. (2012b). Investigating the principles of morphogen gradient formation: from tissues to cells. *Curr. Opin. Genet. Dev.* **22**, 527-532.
Kornberg, T. B. (2012). The imperatives of context and contour for morphogen dispersion. *Biophys. J.* **103**, 2252-2256.
Kornberg, T. B. and Guha, A. (2007). Understanding morphogen gradients: a problem of dispersion and containment. *Curr. Opin. Genet. Dev.* **17**, 264-271.
Kress, H., Stelzer, E. H., Holzer, D., Buss, F., Griffiths, G. and Rohrbach, A. (2007). Filopodia act as phagocytic tentacles and pull with discrete steps and a load-dependent velocity. *Proc. Natl. Acad. Sci. USA* **104**, 11633-11638.
Kruse, K., Pantazis, P., Bollenbach, T., Jülicher, F. and González-Gaitán, M. (2004). Dpp gradient formation by dynamin-dependent endocytosis: receptor trafficking and the diffusion model. *Development* **131**, 4843-4856.
Lander, A. D., Nie, Q. and Wan, F. Y. (2002). Do morphogen gradients arise by diffusion? *Dev. Cell* **2**, 785-796.
Le Good, J. A., Joubin, K., Giraldez, A. J., Ben-Haim, N., Beck, S., Chen, Y., Schier, A. F. and Constam, D. B. (2005). Nodal stability determines signaling range. *Curr. Biol.* **15**, 31-36.
Lecuit, T. and Cohen, S. M. (1998). Dpp receptor levels contribute to shaping the Dpp morphogen gradient in the Drosophila wing imaginal disc. *Development* **125**, 4901-4907.
Lecuit, T., Brook, W. J., Ng, M., Calleja, M., Sun, H. and Cohen, S. M. (1996). Two distinct mechanisms for long-range patterning by Decapentaplegic in the Drosophila wing. *Nature* **381**, 387-393.
Lehmann, M. J., Sherer, N. M., Marks, C. B., Pypaert, M. and Mothes, W. (2005). Actin- and myosin-driven movement of viruses along filopodia precedes their entry into cells. *J. Cell Biol.* **170**, 317-325.
Lidke, D. S., Nagy, P., Heintzmann, R., Arndt-Jovin, D. J., Post, J. N., Grecco, H. E., Jares-Erijman, E. A. and Jovin, T. M. (2004). Quantum dot ligands provide new insights into erbB/HER receptor-mediated signal transduction. *Nat. Biotechnol.* **22**, 198-203.
Lidke, D. S., Lidke, K. A., Rieger, B., Jovin, T. M. and Arndt-Jovin, D. J. (2005). Reaching out for signals: filopodia sense EGF and respond by directed retrograde transport of activated receptors. *J. Cell Biol.* **170**, 619-626.
Lin, X. (2004). Functions of heparan sulfate proteoglycans in cell signaling during development. *Development* **131**, 6009-6021.
Lippincott-Schwartz, J., Altan-Bonnet, N. and Patterson, G. H. (2003). Photobleaching and photoactivation: following protein dynamics in living cells. *Nat. Cell Biol. Suppl.* S7-S14.
Little, S. C., Tkačik, G., Kneeland, T. B., Wieschaus, E. F. and Gregor, T. (2011). The formation of the Bicoid morphogen gradient requires protein movement from anteriorly localized mRNA. *PLoS Biol.* **9**, e1000596.
Liu, W. and Niranjan, M. (2011). The role of regulated mRNA stability in establishing bicoid morphogen gradient in Drosophila embryonic development. *PLoS ONE* **6**, e24896.
Locke, M. (1987). The very rapid induction of filopodia in insect cells. *Tissue Cell* **19**, 301-318.
Makarenkova, H. P., Hoffman, M. P., Beenken, A., Eliseenkova, A. V., Meech, R., Tsau, C., Patel, V. N., Lang, R. A. and Mohammadi, M. (2009). Differential interactions of FGFs with heparan sulfate control gradient formation and branching morphogenesis. *Sci. Signal.* **2**, ra55.
Makhijani, K., Kalyani, C., Srividya, T. and Shashidhara, L. S. (2007). Modulation of Decapentaplegic gradient during haltere specification in Drosophila. *Dev. Biol.* **302**, 243-255.
Marjoram, L. and Wright, C. (2011). Rapid differential transport of Nodal and Lefty on sulfated proteoglycan-rich extracellular matrix regulates left-right asymmetry in Xenopus. *Development* **138**, 475-485.
Matsuda, S. and Shimmi, O. (2012). Directional transport and active retention of Dpp/BMP create wing vein patterns in Drosophila. *Dev. Biol.* **366**, 153-162.
Meinhardt, H. (2004). Different strategies for midline formation in bilaterians. *Nat. Rev. Neurosci.* **5**, 502-510.
Meno, C., Saijoh, Y., Fujii, H., Ikeda, M., Yokoyama, T., Yokoyama, M., Toyoda, Y. and Hamada, H. (1996). Left-right asymmetric expression of the TGF beta-family member lefty in mouse embryos. *Nature* **381**, 151-155.
Milán, M., Weihe, U., Pérez, L. and Cohen, S. M. (2001). The LRR proteins capricious and Tartan mediate cell interactions during DV boundary formation in the Drosophila wing. *Cell* **106**, 785-794.
Miller, J., Fraser, S. E. and McClay, D. (1995). Dynamics of thin filopodia during sea urchin gastrulation. *Development* **121**, 2501-2511.
Miura, T., Hartmann, D., Kinboshi, M., Komada, M., Ishibashi, M. and Shiota, K. (2009). The cyst-branch difference in developing chick lung results from a different morphogen diffusion coefficient. *Mech. Dev.* **126**, 160-172.
Mizutani, C. M., Nie, Q., Wan, F. Y., Zhang, Y. T., Vilmos, P., Sousa-Neves, R., Bier, E., Marsh, J. L. and Lander, A. D. (2005). Formation of the BMP activity gradient in the Drosophila embryo. *Dev. Cell* **8**, 915-924.
Morgan, T. H. (1901). *Regeneration*. New York, NY: Macmillan.
Morisato, D. (2001). Spätzle regulates the shape of the Dorsal gradient in the Drosophila embryo. *Development* **128**, 2309-2319.
Moussian, B. and Roth, S. (2005). Dorsoventral axis formation in the Drosophila embryo – shaping and transducing a morphogen gradient. *Curr. Biol.* **15**, R887-R899.
Müller, P. and Schier, A. F. (2011). Extracellular movement of signaling molecules. *Dev. Cell* **21**, 145-158.
Müller, P., Rogers, K. W., Jordan, B. M., Lee, J. S., Robson, D., Ramanathan, S. and Schier, A. F. (2012). Differential diffusivity of Nodal and Lefty underlies a reaction-diffusion patterning system. *Science* **336**, 721-724.
Mulligan, K. A., Fuerer, C., Ching, W., Fish, M., Willert, K. and Nusse, R. (2012). Secreted Wingless-interacting molecule (Swim) promotes long-range signaling by maintaining Wingless solubility. *Proc. Natl. Acad. Sci. USA* **109**, 370-377.
Nellen, D., Burke, R., Struhl, G. and Basler, K. (1996). Direct and long-range action of a DPP morphogen gradient. *Cell* **85**, 357-368.
Nicholson, C. (2001). Diffusion and related transport mechanisms in brain tissue. *Rep. Prog. Phys.* **64**, 815-884.
Nicholson, C. and Syková, E. (1998). Extracellular space structure revealed by diffusion analysis. *Trends Neurosci.* **21**, 207-215.
Nowak, M., Machate, A., Yu, S. R., Gupta, M. and Brand, M. (2011). Interpretation of the FGF8 morphogen gradient is regulated by endocytic trafficking. *Nat. Cell Biol.* **13**, 153-158.
Panganiban, G. E., Rashka, K. E., Neitzel, M. D. and Hoffmann, F. M. (1990a). Biochemical characterization of the Drosophila dpp protein, a member of the transforming growth factor beta family of growth factors. *Mol. Cell. Biol.* **10**, 2669-2677.
Panganiban, G. E., Reuter, R., Scott, M. P. and Hoffmann, F. M. (1990b). A Drosophila growth factor homolog, decapentaplegic, regulates homeotic gene expression within and across germ layers during midgut morphogenesis. *Development* **110**, 1041-1050.
Pearson, K. (1905a). The problem of the random walk. *Nature* **72**, 294.
Pearson, K. (1905b). The problem of the random walk. *Nature* **72**, 342.
Peng, Y., Han, C. and Axelrod, J. D. (2012). Planar polarized protrusions break the symmetry of EGFR signaling during Drosophila bract cell fate induction. *Dev. Cell* **23**, 507-518.
Porcher, A. and Dostatni, N. (2010). The bicoid morphogen system. *Curr. Biol.* **20**, R249-R254.
Porcher, A., Abu-Arish, A., Huart, S., Roelens, B., Fradin, C. and Dostatni, N. (2010). The time to measure positional information: maternal hunchback is required for the synchrony of the Bicoid transcriptional response at the onset of zygotic transcription. *Development* **137**, 2795-2804.
Ramírez-Weber, F. A. and Kornberg, T. B. (1999). Cytonemes: cellular processes that project to the principal signaling center in Drosophila imaginal discs. *Cell* **97**, 599-607.

Ramírez-Weber, F. A. and Kornberg, T. B. (2000). Signaling reaches to new dimensions in Drosophila imaginal discs. *Cell* **103**, 189-192.
Rayleigh, W. J. S. (1905). The problem of the random walk. *Nature* **72**, 318.
Reeves, G. T. and Stathopoulos, A. (2009). Graded dorsal and differential gene regulation in the Drosophila embryo. *Cold Spring Harb. Perspect. Biol.* **1**, a000836.
Renaud, O. and Simpson, P. (2001). Scabrous modifies epithelial cell adhesion and extends the range of lateral signalling during development of the spaced bristle pattern in Drosophila. *Dev. Biol.* **240**, 361-376.
Reversade, B. and De Robertis, E. M. (2005). Regulation of ADMP and BMP2/4/7 at opposite embryonic poles generates a self-regulating morphogenetic field. *Cell* **123**, 1147-1160.
Ries, J. and Schwille, P. (2012). Fluorescence correlation spectroscopy. *BioEssays* **34**, 361-368.
Rogers, K. W. and Schier, A. F. (2011). Morphogen gradients: from generation to interpretation. *Annu. Rev. Cell Dev. Biol.* **27**, 377-407.
Rojas-Ríos, P., Guerrero, I. and González-Reyes, A. (2012). Cytoneme-mediated delivery of hedgehog regulates the expression of bone morphogenetic proteins to maintain germline stem cells in Drosophila. *PLoS Biol.* **10**, e1001298.
Rørth, P. (2003). Communication by touch: role of cellular extensions in complex animals. *Cell* **112**, 595-598.
Roy, S. and Kornberg, T. B. (2011). Direct delivery mechanisms of morphogen dispersion. *Sci. Signal.* **4**, pt8.
Roy, S., Hsiung, F. and Kornberg, T. B. (2011). Specificity of Drosophila cytonemes for distinct signaling pathways. *Science* **332**, 354-358.
Rusakov, D. A. and Kullmann, D. M. (1998). Geometric and viscous components of the tortuosity of the extracellular space in the brain. *Proc. Natl. Acad. Sci. USA* **95**, 8975-8980.
Sakuma, R., Ohnishi Yi, Y., Meno, C., Fujii, H., Juan, H., Takeuchi, J., Ogura, T., Li, E., Miyazono, K. and Hamada, H. (2002). Inhibition of Nodal signalling by Lefty mediated through interaction with common receptors and efficient diffusion. *Genes Cells* **7**, 401-412.
Sample, C. and Shvartsman, S. Y. (2010). Multiscale modeling of diffusion in the early Drosophila embryo. *Proc. Natl. Acad. Sci. USA* **107**, 10092-10096.
Sankaran, J., Shi, X., Ho, L. Y., Stelzer, E. H. and Wohland, T. (2010). ImFCS: a software for imaging FCS data analysis and visualization. *Opt. Express* **18**, 25468-25481.
Sato, M. and Kornberg, T. B. (2002). FGF is an essential mitogen and chemoattractant for the air sacs of the drosophila tracheal system. *Dev. Cell* **3**, 195-207.
Saunders, T. E., Pan, K. Z., Angel, A., Guan, Y., Shah, J. V., Howard, M. and Chang, F. (2012). Noise reduction in the intracellular pom1p gradient by a dynamic clustering mechanism. *Dev. Cell* **22**, 558-572.
Sawala, A., Sutcliffe, C. and Ashe, H. L. (2012). Multistep molecular mechanism for bone morphogenetic protein extracellular transport in the Drosophila embryo. *Proc. Natl. Acad. Sci. USA* **109**, 11222-11227.
Schier, A. F. (2009). Nodal morphogens. *Cold Spring Harb. Perspect. Biol.* **1**, a003459.
Schilling, T. F., Nie, Q. and Lander, A. D. (2012). Dynamics and precision in retinoic acid morphogen gradients. *Curr. Opin. Genet. Dev.* **22**, 562-569.
Scholpp, S. and Brand, M. (2004). Endocytosis controls spreading and effective signaling range of Fgf8 protein. *Curr. Biol.* **14**, 1834-1841.
Schwank, G., Dalessi, S., Yang, S. F., Yagi, R., de Lachapelle, A. M., Affolter, M., Bergmann, S. and Basler, K. (2011). Formation of the long range Dpp morphogen gradient. *PLoS Biol.* **9**, e1001111.
Shimmi, O., Umulis, D., Othmer, H. and O'Connor, M. B. (2005). Facilitated transport of a Dpp/Scw heterodimer by Sog/Tsg leads to robust patterning of the Drosophila blastoderm embryo. *Cell* **120**, 873-886.
Spirov, A., Fahmy, K., Schneider, M., Frei, E., Noll, M. and Baumgartner, S. (2009). Formation of the bicoid morphogen gradient: an mRNA gradient dictates the protein gradient. *Development* **136**, 605-614.
Sprague, B. L. and McNally, J. G. (2005). FRAP analysis of binding: proper and fitting. *Trends Cell Biol.* **15**, 84-91.
Stewart, I. (2001). Mathematics. Where drunkards hang out. *Nature* **413**, 686-687.
Stumpf, H. F. (1966). Mechanism by which cells estimate their location within the body. *Nature* **212**, 430-431.
Sui, L., Pflugfelder, G. O. and Shen, J. (2012). The Dorsocross T-box transcription factors promote tissue morphogenesis in the Drosophila wing imaginal disc. *Development* **139**, 2773-2782.
Swaney, K. F., Huang, C. H. and Devreotes, P. N. (2010). Eukaryotic chemotaxis: a network of signaling pathways controls motility, directional sensing, and polarity. *Annu. Rev. Biophys.* **39**, 265-289.
Takei, Y., Ozawa, Y., Sato, M., Watanabe, A. and Tabata, T. (2004). Three Drosophila EXT genes shape morphogen gradients through synthesis of heparan sulfate proteoglycans. *Development* **131**, 73-82.
Tao, L. and Nicholson, C. (2004). Maximum geometrical hindrance to diffusion in brain extracellular space surrounding uniformly spaced convex cells. *J. Theor. Biol.* **229**, 59-68.
Teleman, A. A. and Cohen, S. M. (2000). Dpp gradient formation in the Drosophila wing imaginal disc. *Cell* **103**, 971-980.
Tenlen, J. R., Molk, J. N., London, N., Page, B. D. and Priess, J. R. (2008). MEX-5 asymmetry in one-cell C. elegans embryos requires PAR-4- and PAR-1-dependent phosphorylation. *Development* **135**, 3665-3675.
Thiele, E. W. (1939). Relation between catalytic activity and size of particle. *Ind. Eng. Chem.* **31**, 916-920.
Thorne, R. G. and Nicholson, C. (2006). In vivo diffusion analysis with quantum dots and dextrans predicts the width of brain extracellular space. *Proc. Natl. Acad. Sci. USA* **103**, 5567-5572.
Thorne, R. G., Lakkaraju, A., Rodriguez-Boulan, E. and Nicholson, C. (2008). In vivo diffusion of lactoferrin in brain extracellular space is regulated by interactions with heparan sulfate. *Proc. Natl. Acad. Sci. USA* **105**, 8416-8421.
Tian, J., Andrée, B., Jones, C. M. and Sampath, K. (2008). The pro-domain of the zebrafish Nodal-related protein Cyclops regulates its signaling activities. *Development* **135**, 2649-2658.
Tukachinsky, H., Kuzmickas, R. P., Jao, C. Y., Liu, J. and Salic, A. (2012). Dispatched and scube mediate the efficient secretion of the cholesterol-modified hedgehog ligand. *Cell Rep.* **2**, 308-320.
Turing, A. M. (1952). The chemical basis of morphogenesis. *Phil. Trans. R. Soc. Lond. B* **237**, 37-72.
Umulis, D., O'Connor, M. B. and Blair, S. S. (2009). The extracellular regulation of bone morphogenetic protein signaling. *Development* **136**, 3715-3728.
van der Zee, M., Stockhammer, O., von Levetzow, C., Nunes da Fonseca, R. and Roth, S. (2006). Sog/Chordin is required for ventral-to-dorsal Dpp/BMP transport and head formation in a short germ insect. *Proc. Natl. Acad. Sci. USA* **103**, 16307-16312.
Vasioukhin, V., Bauer, C., Yin, M. and Fuchs, E. (2000). Directed actin polymerization is the driving force for epithelial cell-cell adhesion. *Cell* **100**, 209-219.
Vitriol, E. A. and Zheng, J. Q. (2012). Growth cone travel in space and time: the cellular ensemble of cytoskeleton, adhesion, and membrane. *Neuron* **73**, 1068-1081.
Wang, Y. C. and Ferguson, E. L. (2005). Spatial bistability of Dpp-receptor interactions during Drosophila dorsal-ventral patterning. *Nature* **434**, 229-234.
Wang, X., Harris, R. E., Bayston, L. J. and Ashe, H. L. (2008). Type IV collagens regulate BMP signalling in Drosophila. *Nature* **455**, 72-77.
Wartlick, O., Kicheva, A. and González-Gaitán, M. (2009). Morphogen gradient formation. *Cold Spring Harb. Perspect. Biol.* **1**, a001255.
Wartlick, O., Mumcu, P., Kicheva, A., Bittig, T., Seum, C., Jülicher, F. and González-Gaitán, M. (2011). Dynamics of Dpp signaling and proliferation control. *Science* **331**, 1154-1159.
Wohland, T., Shi, X., Sankaran, J. and Stelzer, E. H. (2010). Single plane illumination fluorescence correlation spectroscopy (SPIM-FCS) probes inhomogeneous three-dimensional environments. *Opt. Express* **18**, 10627-10641.
Wolf, C., Gerlach, N. and Schuh, R. (2002). Drosophila tracheal system formation involves FGF-dependent cell extensions contacting bridge-cells. *EMBO Rep.* **3**, 563-568.
Wolpert, L. (1969). Positional information and the spatial pattern of cellular differentiation. *J. Theor. Biol.* **25**, 1-47.
Wolpert, L. (2009). Diffusible gradients are out - an interview with Lewis Wolpert. Interviewed by Richardson, Michael K. *Int. J. Dev. Biol.* **53**, 659-662.
Yan, D. and Lin, X. (2009). Shaping morphogen gradients by proteoglycans. *Cold Spring Harb. Perspect. Biol.* **1**, a002493.
Yu, S. R., Burkhardt, M., Nowak, M., Ries, J., Petrásek, Z., Scholpp, S., Schwille, P. and Brand, M. (2009). Fgf8 morphogen gradient forms by a source-sink mechanism with freely diffusing molecules. *Nature* **461**, 533-536.
Yuste, R. and Bonhoeffer, T. (2004). Genesis of dendritic spines: insights from ultrastructural and imaging studies. *Nat. Rev. Neurosci.* **5**, 24-34.
Zhou, X., Sasaki, H., Lowe, L., Hogan, B. L. and Kuehn, M. R. (1993). Nodal is a novel TGF-beta-like gene expressed in the mouse node during gastrulation. *Nature* **361**, 543-547.
Zhou, S., Lo, W. C., Suhalim, J. L., Digman, M. A., Gratton, E., Nie, Q. and Lander, A. D. (2012). Free extracellular diffusion creates the Dpp morphogen gradient of the Drosophila wing disc. *Curr. Biol.* **22**, 668-675.